RAA 2019 Vol. **19** No. **1**, 1(20pp) doi: 10.1088/1674–4527/19/1/1

http://www.raa-journal.org *http://iopscience.iop.org/raa*

***R**esearch in*
***A**stronomy and*
***A**strophysics*

EDITOR'S RECOMMENDATION

Physical properties of γ Doradus pulsating stars and their relationship with long-period δ Scuti variables

Sheng-Bang Qian[1,2,3,4], Lin-Jia Li[1,2,3], Jia-Jia He[1,2,3], Jia Zhang[1,2,3], Li-Ying Zhu[1,2,3,4] and Zhong-Tao Han[1,2,3]

[1] Yunnan Observatories, Chinese Academy of Sciences, Kunming 650216, China; *qsb@ynao.ac.cn*
[2] Key Laboratory of the Structure and Evolution of Celestial Objects, Chinese Academy of Sciences, Kunming 650216, China
[3] Center for Astronomical Mega-Science, Chinese Academy of Sciences, Beijing 100101, China
[4] University of Chinese Academy of Sciences, Beijing 100049, China

Received 2018 November 30; accepted 2018 December 6

Abstract We present LAMOST data on 168 γ Doradus (γ Dor) pulsating stars including stellar atmospheric parameters of 137 variables and spectral types for all of the samples. The distributions of period (P), temperature (T), gravitational acceleration ($\log(g)$) and metallicity [Fe/H] are shown. It is found that most γ Dor variables are main-sequence stars with early F spectral types and temperatures from 6880 K to 7280 K. They are slightly more metal poor than the Sun with a metallicity range from -0.4 to 0. On the H-R and $\log g - T$ diagrams, both the γ Dor and δ Scuti (δ Sct) stars occupy in the same region and some are beyond the borders predicted by current stellar pulsation theories. It is discovered that the physical properties of γ Dor stars are similar to those of long-period δ Sct ($P > 0.3$ d) stars. The stellar atmospheric parameters are all correlated with the pulsation period for short-period δ Sct variables ($P < 0.3$ d), but there are no such relations for γ Dor or long-period δ Sct stars. These results reveal that γ Dor and long-period δ Sct are the same group of pulsating stars and they are different from short-period δ Sct variables. Meanwhile, 33 γ Dor stars are identified as candidates of binary or multiple systems.

Key words: stars: fundamental parameters — stars: oscillations — stars: binaries: spectroscopic — stars: variables: other

1 INTRODUCTION

γ Doradus (γ Dor) stars are a class of main-sequence variables that were identified about two decades ago (e.g., Krisciunas et al. 1993; Balona et al. 1994; Mantegazza et al. 1994; Krisciunas & Handler 1995). The prototype of this class of variable star, γ Dor, is an early-F pulsator that was detected as a variable star by Cousins & Warren (1963). This type of variable pulsates with multiple photometric periods between 0.3 and 3 d and has sinusoidal light curves with amplitudes of a few mmag to a few percent (e.g., Henry et al. 2005, 2007). Their spectral types are in the range from A7 to F5 ($7400 > T > 6900$ K) with luminosity class IV-V or V (e.g., Kaye et al. 1999). On the Hertzsprung-Russell (H-R) diagram, the instability strip of γ Dor stars is rather narrow. They lie in the lower part of the classical instability strip that partially overlaps the cool edge of the δ Scuti (δ Sct) instability strip (Handler 1999). Their gravity (g) modes are thought to be driven by the convective blocking mechanism (Guzik et al. 2000; Dupret et al. 2005; Grigahcène et al. 2005).

The relationship between γ Dor and δ Sct pulsating stars is an interesting question (Breger & Beichbuchner 1996; Handler & Shobbrook 2002). The overlap around the red edge of instability strips for these two types of variables suggests the possibility that some stars might show both δ Sct and γ Dor (so-called hybrid) pulsation behavior. Such hybrid stars provide a unique opportunity for asteroseismology because the g-modes observed in γ Dor

could probe the stellar core, whereas the p-modes could probe the envelope. Several hybrid stars such as HD 8801 (Henry & Fekel 2005; Handler 2009), HD 44195 (Poretti et al. 2005), HD 49434 (Uytterhoeven et al. 2008) and GSC3382-0957 (Zhang et al. 2012) were detected from ground-based observations. However, many hybrid stars were identified from space missions (e.g., Grigahcène et al. 2010; Catanzaro et al. 2011; Balona 2014; Bradley et al. 2015). It is interesting that some hybrid stars are members of close binaries such as KIC 6048106 (Samadi Ghadim et al. 2018) and KIC 9851944 (Guo et al. 2016). Some investigators thought that the driving mechanism of the two classes should be different because of the different types of modes excited. δ Sct pulsations are driven by the κ mechanism (e.g., Handler 1999), while the driving mechanism for γ Dor stars is similar to convective blocking (Guzik et al. 2000; Dupret et al. 2005). However, a recent investigation by Xiong et al. (2016) indicated that pulsations of δ Sct and γ Dor stars are both due to the combination of the κ mechanism and coupling between convection and oscillations. They pointed out that the two types of pulsating stars belong to the same class of variables at the low-luminosity part of the Cepheid instability strip.

More than 100 γ Dor pulsators were identified from ground-based observations (e.g., Handler 1999; Henry et al. 2005, 2011). Many observing campaigns targeting individual γ Dor stars have confirmed their high-order and non-radial g-mode pulsations (e.g., Aerts et al. 2004; Rodríguez et al. 2006). However, γ Dor variables are hard to detect from the ground because of the relatively low amplitude and long period of pulsations. In the new catalog recently published by Ibanoglu et al. (2018), ground-based γ Dor stars are usually brighter than 10 magnitude. Space telescopes such as *MOST* (Walker et al. 2003), *CoRoT* (Baglin et al. 2006) and *Kepler* (Borucki et al. 2010) do not suffer these limitations. Those long-term and highly-precise photometric observations open a new window towards understanding the seismic behavior of γ Dor. About 291 and 307 γ Dor pulsators were detected by *CoRoT* and *Kepler* (e.g., Sarro et al. 2013; Grigahcène et al. 2010; Uytterhoeven et al. 2011; Tkachenko et al. 2013; Bradley et al. 2015), respectively. Unfortunately, because of the relatively low declinations of the *CoRoT* targets (declination lower than 8 degrees), most of them are not suitable to be observed by the Large Sky Area Multi-object Fiber Spectroscopic Telescope (LAMOST). Since observations of variable stars including γ Dor pulsating stars are constantly varying, the goal of the International Variable Star Index (VSX) is to compile new data together in a single data repository (e.g., Watson et al. 2006). About 400 γ Dor pulsating stars were listed in VSX by 2017 July 16. Photometric data from space missions are very useful and provide valuable information on the physical properties of γ Dor stars. However, their spectroscopic information including stellar atmospheric parameters as well as spectral types is extremely lacking.

LAMOST is a special telescope with an aperture of about 4 meters that is used for spectroscopic surveys (Wang et al. 1996; Cui et al. 2012). The field of view for LAMOST is about 5 degrees and it can acquire spectra of about 4000 stars in one exposure. Huge amounts of spectroscopic observations were obtained for single stars and binary systems (e.g., Zhao et al. 2012; Luo et al. 2015; Qian et al. 2017, 2018a,b). In the time interval between 2011 October 24 and 2017 July 16, about 168 γ Dor pulsating stars were observed by LAMOST. Since the LAMOST targets are usually fainter than 9 magnitude, most of the observed γ Dor variables were detected with space telescopes, especially *Kepler*. In the most recent LAMOST data releases (DR4 and the first three quarters of DR5), 255 sets of stellar atmospheric parameters for 137 γ Dor stars were determined when their spectra had higher signal to noise ratio, and spectral types of all 168 variables were obtained. Those data could give us valuable information on the physical properties, evolutionary states, classifications and binarities for this type of pulsating star.

In DR4 and the first three quarters of DR5, about 42% of γ Dor stars in VSX were observed by the LAMOST survey from 2011 October 24 to 2017 July 16. The periods of the 168 samples are provided in VSX. The period distribution for those observed pulsating stars is shown in Figure 1 as blue dots. Also plotted in the figure, as green ones, is the period distribution of all γ Dor stars in VSX where nine variables without orbital periods are not displayed. As displayed in the figure, the peak of the period distribution is in the range from 0.4 to 0.6 d (the two red dashed lines). The number of γ Dor stars is rapidly decreasing when the period is shorter than 0.4 d. In the paper, spectroscopic data obtained by the LAMOST survey are presented. Then, based on the distributions of those atmospheric parameters and some statistical correlations, the physical properties, classification, evolutionary states and binarities of γ Dor pulsating stars are discussed.

2 CATALOG OF γ DOR STARS OBSERVED BY LAMOST

In the latest LAMOST data (DR4 and the first three quarters of DR5), about 168 γ Dor stars listed in the VSX catalog were observed by the LAMOST spectroscopic sur-

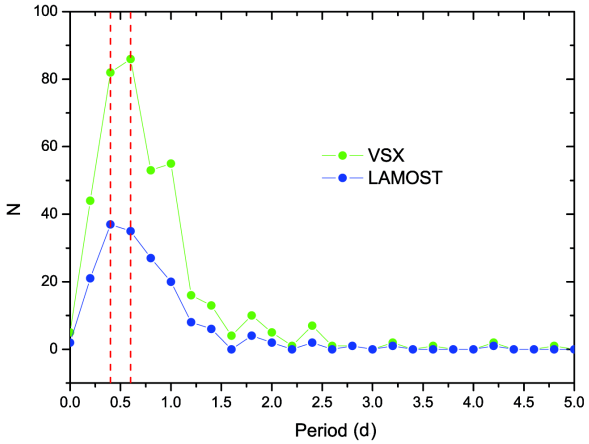

Fig. 1 Period distribution of γ Dor stars observed by LAMOST (*blue dots*). Also shown as *green dots* are all γ Dor pulsating stars listed in the VSX catalog. The *red dashed lines* indicate that most γ Dor variables are in the period range from 0.4 to 0.6 d.

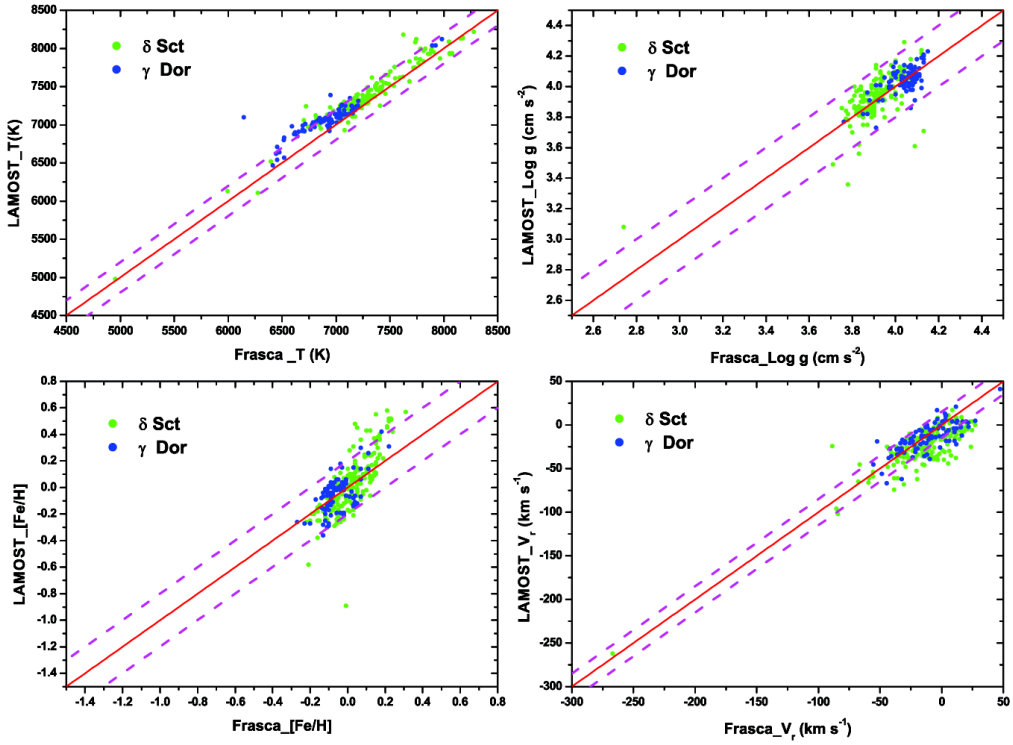

Fig. 2 Comparison between LASP data of LAMOST-*Kepler* γ Dor stars (*blue dots*) and stellar atmospheric parameters derived with ROTFIT from the LAMOST spectra by Frasca et al. (2016). The *red solid lines* in the four panels are one-to-one relationships. The *dashed magenta lines* refer to a difference of 200 K for T, 0.2 for $\log(g)$ and [Fe/H], and 15 km s^{-1} for $V_{\rm r}$, in the corresponding panels. Also shown in the four panels as *green dots* are δ Sct stars in the LAMOST-*Kepler* field.

vey from 2011 October 24 to 2017 June 16. Among the 168 γ Dor stars, the stellar atmospheric parameters including effective temperature T, gravitational acceleration $\log(g)$, metallicity [Fe/H] and radial velocity $V_{\rm r}$ were determined for 137 variables, while only spectral types were obtained for the other ones. Those stellar atmospheric parameters were automatically determined by the LAMOST stellar parameter pipeline when their spectra had higher signal to noise ratio (e.g., Wu et al. 2011b, 2014; Luo et al. 2015). They were derived based on the Universite de Lyon Spectroscopic analysis Software (ULySS) (e.g., Koleva et al. 2009; Wu et al. 2011a). All the observed LAMOST spectra were fitted by using model spectra that were generated by an interpolator that employed the

ELODIE library as a reference (e.g., Prugniel & Soubiran 2001). Atmospheric parameters of 352 stars were derived by Frasca et al. (2016) from high-resolution optical spectra in the literature. Qian et al. (2018a) have compared the recently released data with those determined by Frasca et al. (2016). It is shown that they are in very good agreement and the standard deviations are 135 K for T, 0.21 dex for $\log g$, 0.14 dex for [Fe/H] and 11 km s^{-1} for $V_{\rm r}$.

More than 300 γ Dor stars were detected by the *Kepler* space telescope (e.g., Grigahcène et al. 2010; Uytterhoeven et al. 2011; Tkachenko et al. 2013; Bradley et al. 2015). Some of those γ Dor stars in the *Kepler* field of view were also observed by the LAMOST spectroscopic survey in the time interval between 2011 October 24 and 2017 June 16. By using LAMOST spectra, the stellar atmospheric parameters of *Kepler*-field stars were also derived by Frasca et al. (2016) with the code ROTFIT that was developed by Frasca et al. (2003, 2006). Atmospheric parameters for 111 γ Dor stars were determined. To check the LAMOST Stellar Parameter Pipeline (LASP, Luo et al. 2015) data (DR4 and the first three quarters of DR5), the present atmospheric parameters of the 111 γ Dor stars are compared with those derived with ROTFIT. They are shown as blue dots in Figure 2. The red solid lines in the four panels of Figure 2 represent one-to-one relationships. Also shown as green dots in those panels are the 188 LAMOST-*Kepler* δ Sct stars given by Qian et al. (2018a). The dashed magenta lines refer to a difference of 200 K for T, 0.2 for $\log g$ and [Fe/H], and 15 km s^{-1} for $V_{\rm r}$. As evident in the four panels, most γ Dor stars are within the differences, indicating that LASP values are in good agreement with those determined by using ROTFIT.

Like those δ Sct stars investigated by Qian et al. (2018a), the temperatures of all γ Dor variables are below 8500 K, and their atmospheric parameters could be derived well. There are 12 γ Dor stars that were observed four times or more. To check their reliability, we derived the mean values of those stellar atmospheric parameters and determined their standard errors. The corresponding results are displayed in Table 1. Shown in the first and second columns are the names and periods of those γ Dor variables respectively. The observational times are listed in the third column, while the mean atmospheric parameters and the corresponding standard errors are shown in the other columns of the table. As we can see in Table 1, the standard errors of effective temperature for all γ Dor stars are lower than 70 K, while the standard errors of gravitational acceleration $\log(g)$ are lower than 0.04 dex. Apart from one target, the standard errors of metallicity for the other targets are lower than 0.06 dex.

Two-hundred fifty-five sets of stellar atmospheric parameters for 137 γ Dor stars are shown in Table 2 in order of increasing VSX number. Some γ Dor variables were observed two or more times on different dates and we list all of the original observations. Table 2 includes the names of those γ Dor stars, their right ascensions (R.A.) and declinations (Dec.), types of light variation and periods. All of these parameters are from the VSX catalog. The types of light variation are from the GCVS variability classification scheme[1] (e.g., Samus' et al. 2017). Values listed in column 6 are the distances (in arcsec) between the two positions derived with coordinates given in VSX and by LAMOST. As done for EW and EA binaries (Qian et al. 2017, 2018b), the distances were used to identify γ Dor stars from the LAMOST samples based on the criterion Dist$<$ 2 arcsecs. The observing dates and determined spectral types of those γ Dor variables are shown in columns 7 and 8. The stellar atmospheric parameters (T, $\log(g)$, [Fe/H] and $V_{\rm r}$) of 137 γ Dor stars are listed in columns 9, 11, 13 and 15, while their corresponding errors E_1, E_2, E_3 and E_4 are shown in columns 10, 12, 14 and 16, respectively.

The relative distribution (the percentage of the number to the whole sample) of the orbital period for 137 γ Dor stars is displayed in Figure 3. For comparison, the relative period distribution of all γ Dor variables in VSX is also shown in the figure. It is found that both of them nearly overlap. This indicates that those 137 γ Dor stars could be used to represent the properties of all the γ Dor stars in the whole VSX catalog. As shown in Figures 1 and 3, the period distribution peaks are in the range from 0.4 to 0.6 d (the red dashed line). The number of γ Dor stars rapidly decreases with periods shorter than 0.4 d. A long tail extends beyond 1.5 d, in fact to about 3 d.

For some LAMOST spectra of γ Dor stars, their signal to noise ratios are not high enough to determine the stellar atmospheric parameters. In these cases, only spectral types are given. The spectral types of those γ Dor stars are shown in Table 3 in order of increasing VSX number. Table 3 lists 104 spectral types. The descriptions of those columns are the same as those in Table 2.

3 DISTRIBUTIONS OF STELLAR ATMOSPHERIC PARAMETERS AND BINARITIES FOR OBSERVED γ DOR STARS

Stellar atmospheric parameters of 137 γ Dor stars were obtained by LAMOST from 2011 October 24 to 2017 June 16. In this section, we investigate the physical properties of γ Dor stars by using those data. As displayed in Figure 3,

[1] *http://www.sai.msu.su//gcvs/gcvs/iii/vartype.txt*

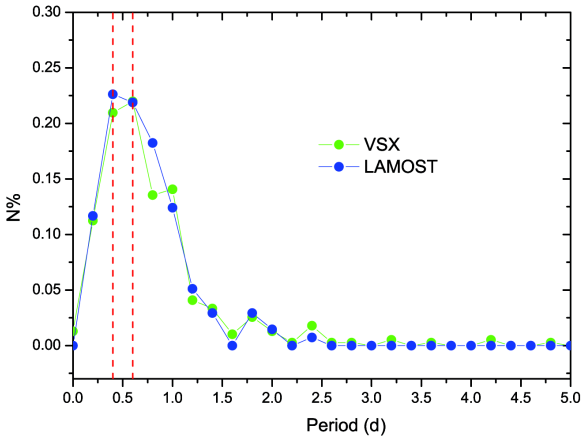

Fig. 3 The relative distributions of pulsation period for γ Dor stars observed by LAMOST and listed in VSX. The *red dashed lines* indicate that the peak is around 0.4–0.6 d. Symbols are the same as those in Fig. 1.

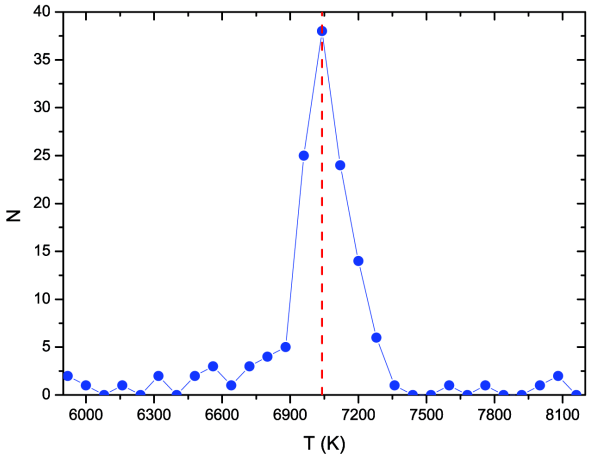

Fig. 4 Distribution of the effective temperature for 137 γ Dor stars whose stellar atmospheric parameters were derived by LAMOST. The *dashed line* refers to the peak near 7040 K.

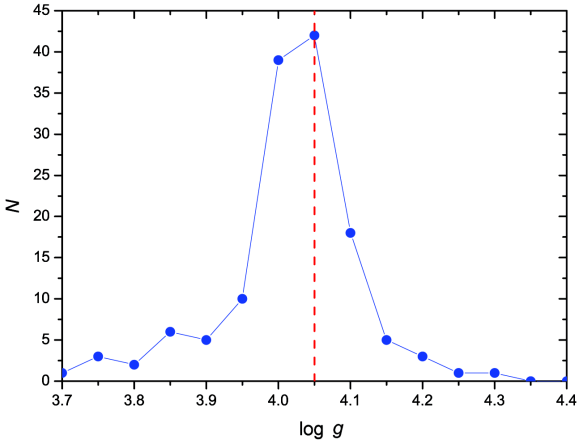

Fig. 5 The distribution of gravitational acceleration $\log(g)$ for observed γ Dor stars. The peak is near 4.05.

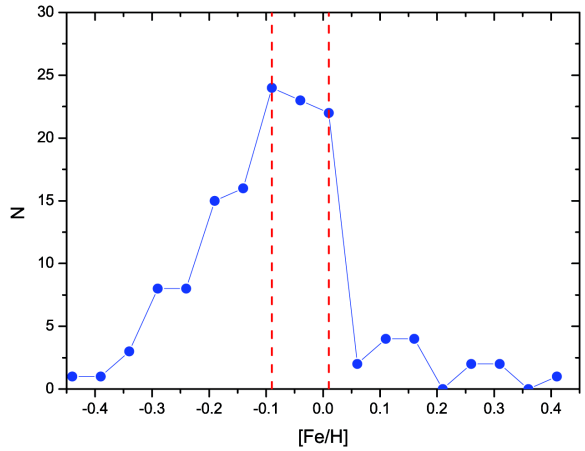

Fig. 6 The distribution of metallicity [Fe/H] for 137 observed γ Dor stars. The peak is between [Fe/H]$= -0.09$ and 0.01.

Table 1 Mean Atmospheric Parameters for 12 γ Dor Stars Observed Four Times or More and Their Standard Errors

Star Name	P (d)	Times	$\overline{T_{\rm eff}}$(K)	Errors	$\overline{\log(g)}$	Errors	$\overline{[{\rm Fe/H}]}$	Errors
KIC 11456474	0.6796	9	6985.23	34.05	4.043	0.014	–0.093	0.023
KIC 7023122	0.533	6	7219.55	28.36	4.098	0.006	–0.19	0.008
KID 6869740	0.3517	5	7086.8	10.78	4.002	0.037	0.048	0.012
KIC 7436266	0.58343	5	6998.89	51.02	4.036	0.02	–0.068	0.04
KIC 10586837	0.63735	5	7075.62	7.83	3.991	0.032	–0.076	0.06
KIC 10652134	1.30548	5	7026.67	6.31	4.026	0.015	–0.06	0.126
KIC 5724048	0.46926	4	6542.87	48.77	4.217	0.019	–0.263	0.009
KIC 11080103	0.8055	4	7107.36	60.91	4.108	0.015	–0.311	0.041
KIC 3441414	0.81072	4	7083.28	12.39	4.04	0.007	–0.128	0.02

the relative period distribution for those observed γ Dor variables (i.e., the percentage of the number of cases to the whole sample) is nearly the same as that of all γ Dor stars in VSX. Therefore, they could be used to represent the physical properties of all the γ Dor stars listed in the whole VSX catalog. During the analyses, the stellar atmospheric parameters including the effective temperature T, gravitational acceleration $\log(g)$ and metallicity [Fe/H] were averaged when the γ Dor stars were observed twice or more and only the mean values were used. For each datum, its

Table 2 Stellar Atmospheric Parameters for γ Dor Stars Observed by LAMOST

Name	R.A. (deg)	Dec. (deg)	Type	P (d)	Dist	Date	Sp.	T (K)	E_1	$\log(g)$	E_2	[Fe/H]	E_3	$V_{\rm r}$	E_4
NSV 16957	100.02358	9.59703	GDOR	1.488	0.113	2012–2–2	F2	6170	40	3.89	0.05	0.02	0.03	20	4
NSV 18764	171.4092	29.9873	GDOR	0.47549	0.356	2012–1–11	F0	7160	450	4.08	0.64	–0.27	0.42	–27	37
NSV 20738	250.37125	6.27594	GDOR	1.38688	0.008	2017–5–16	A3V	7060.05	2.98	4.21	0.002	–0.512	0.002	10.35	0.65
ASAS J025657+1848.5	44.23679	18.80911	GDOR	1.01077	0.022	2015–10–30	F0	7090	10	4.09	0	–0.03	0	–59	1
V0546 Aur	90.43371	49.94175	GDOR	0.82235	0.492	2015–1–29	F0	7140	150	4.02	0.2	–0.44	0.13	–8	11
HAT 199–01905	294.03762	39.62858	GDOR+DSCT	1.12152	0.067	2017–6–13	A6IV	7254.6	55.89	4.169	0.079	–0.296	0.052	27.13	4.87
HAT 199–07893	291.37179	37.09917	GDOR	0.28977	0.012	2012–6–15	A7III	7150	10	4.01	0.01	0.04	0.01	–13	2
HAT 199–07893	291.37179	37.09917	GDOR	0.28977	0.118	2015–10–12	F0	7170	10	3.97	0	0.02	0	–6	1
NGC 6866 V11	300.99729	44.17383	GDOR	0.740741	0.012	2013–9–25	F0	7190	20	4.08	0.03	–0.21	0.02	4	3
KID 03424493	285.15642	38.50561	GDOR	0.36914	0.065	2017–6–3	A6IV	7382.06	40.68	4.124	0.057	–0.155	0.038	–40.43	3.77
KIC 9595743	294.83011	46.2493	GDOR	0.5781	0.264	2015–9–21	F0	7130	10	4.06	0.01	–0.19	0.01	–23	2
KID 3222854	287.91058	38.34551	GDOR	0.9456	0.004	2017–6–3	F0	7030.69	7.31	4.149	0.009	–0.042	0.007	–40.3	1.12
KID 7731467	281.75612	43.419	GDOR:	1.105	0.111	2015–10–4	F0	6980	10	4.06	0	–0.02	0	–18	1
KID 11759297	289.65104	49.94358	GDOR+DSCT	0.3949	0.396	2015–5–29	F0	7230	10	4.04	0.01	0.13	0.01	3	2
KID 11759297	289.65104	49.94358	GDOR+DSCT	0.3949	0.396	2014–9–17	F0	7250	10	4.08	0	0.15	0	–4	1
KID 11971335	295.67896	50.36341	GDOR:	0.78374	0.004	2015–10–1	G2	6020	10	4.28	0	0.02	0	–6	1
KID 4374526	294.02354	39.45854	GDOR	0.7375	0.139	2015–10–18	F3	6630	20	4.13	0.02	–0.14	0.01	–45	2
KID 08197761	301.03879	44.07111	GDOR	0.91158	0.006	2013–9–25	F0	7140	10	4	0	–0.06	0	–32	1
KID 08355134	287.50671	44.37497	GDOR	0.72727	0.009	2013–10–4	F5	6340	120	4.64	0.16	0.23	0.11	7	10
KID 08355134	287.50671	44.37497	GDOR	0.72727	0.082	2017–6–15	A8III	7086.81	6.23	4.066	0.007	–0.179	0.006	–1.09	1.23
KID 08355134	287.50671	44.37497	GDOR	0.72727	0.082	2015–9–25	F0	7130	10	4.05	0	–0.13	0	9	1
KID 08355134	287.50671	44.37497	GDOR	0.72727	0.149	2016–5–18	F0	7140	10	4.09	0.01	–0.13	0.01	6	2
KID 6869740	293.77217	42.35561	GDOR	0.3517	1.452	2015–10–18	A7III	7070	10	4	0	0.03	0	–39	1
KID 6869740	293.77217	42.35561	GDOR	0.3517	1.452	2014–9–13	F0	7090	10	3.99	0	0.04	0	–31	1
KID 6869740	293.77217	42.35561	GDOR	0.3517	1.452	2014–9–13	F0	7090	10	3.99	0	0.06	0	–28	1
KID 6869740	293.77217	42.35561	GDOR	0.3517	1.452	2015–9–21	F0	7090	70	4.07	0.09	0.04	0.06	–23	6
KID 6869740	293.77217	42.35561	GDOR	0.3517	1.452	2012–6–4	F0	7100	20	3.97	0.02	0.06	0.02	–26	2
KID 9594007	294.20358	46.2415	GDOR	0.6446	0.007	2014–9–13	F0	7090	40	4.08	0.04	–0.2	0.03	–17	4
KID 7661054	282.14604	43.38936	GDOR	1.02	1.045	2017–6–7	F0	6991.43	26.45	3.949	0.036	0.133	0.025	–19.66	2.73
KIC 2300165	290.81992	37.66653	GDOR	0.59559	0.2	2017–6–13	F0	7100.07	6.41	4.109	0.008	–0.216	0.006	–14.22	0.99
KIC 2300165	290.81992	37.66653	GDOR	0.59559	0.2	2015–10–12	F0	7110	10	4.09	0	–0.21	0	–26	1
KIC 2300165	290.81992	37.66653	GDOR	0.59559	0.292	2012–6–15	F0	7140	10	4.1	0	–0.17	0	–22	1
KIC 2568519	290.01642	37.87428	GDOR	1.17925	0.085	2015–10–12	F0	6790	10	4.04	0	–0.12	0	–2	1
KIC 2720582	293.08829	37.98583	GDOR	1.81488	0.012	2012–6–17	F0	7030	50	4.03	0.07	–0.04	0.05	–56	5
KIC 2720582	293.08829	37.98583	GDOR	1.81488	0.032	2015–10–18	F0	7070	10	4.02	0.01	–0.01	0.01	–58	2
KIC 3215800	285.26521	38.30675	GDOR	0.66401	0.287	2016–5–12	F5	6390	20	4.2	0.02	–0.27	0.01	19	2
KIC 3222364	287.74808	38.35553	GDOR	0.4029	0.086	2017–6–3	F0	7096.25	2.3	4.081	0.001	–0.198	0.002	–29.26	0.51
KIC 3327681	287.052	38.48397	GDOR	0.98912	0.089	2017–6–3	F5	6554.01	2.87	4.093	0.002	–0.007	0.002	–53.76	0.63
KIC 3331147	288.28229	38.45953	GDOR	0.70077	0.009	2012–6–15	F0	7090	10	4.09	0	–0.07	0	1	1
KIC 3655608	293.9965	38.74592	GDOR	1.57233	0.011	2012–6–17	F0	6710	90	3.99	0.12	0.14	0.08	–1	7
KIC 3655608	293.9965	38.74592	GDOR	1.57233	0.011	2012–6–15	F0	6770	10	4.03	0.01	0.19	0.01	0	2
KIC 3663141	295.66321	38.71825	GDOR	0.35868	0.088	2017–6–12	F4	6497.27	125.78	4.308	0.179	–0.033	0.117	3.77	9.86
KIC 3663141	295.66321	38.71825	GDOR	0.35868	0.088	2015–10–18	F5	6670	320	4.32	0.44	–0.12	0.29	2	24
KIC 3758717	294.42558	38.85567	GDOR	1.14811	0.03	2017–6–12	F0	6739.01	3.32	4.135	0.003	–0.004	0.003	–30.98	0.69
KIC 3966357	294.60042	39.08303	GDOR	0.62696	0.011	2012–6–17	F0	7120	30	3.98	0.03	0.01	0.02	–27	3
KIC 4069477	294.6605	39.14033	GDOR	0.71023	0.066	2015–10–18	F0	7050	10	4.06	0.01	–0.08	0.01	–24	2
KIC 4069477	294.6605	39.14033	GDOR	0.71023	0.066	2017–6–12	F0	7098.98	2.14	4.049	0.002	–0.071	0.002	–42.74	0.52
KIC 4164363	293.21058	39.24069	GDOR	0.72411	0.144	2015–10–18	F0	7330	10	4.01	0	–0.04	0	–6	1
KIC 4164363	293.21058	39.24069	GDOR	0.72411	0.144	2017–6–12	F0	7336.94	3.88	4.037	0.004	–0.059	0.004	–22.47	0.86
KIC 4758316	294.92371	39.80128	GDOR	1.00908	0.009	2012–6–17	F0	7130	20	4.03	0.02	0.01	0.02	–18	2
KIC 5180796	289.95658	40.32186	GDOR	0.5291	0.028	2015–10–12	A5V	8090	10	3.8	0	–0.04	0	–54	1
KIC 5180796	289.95658	40.32186	GDOR	0.5291	0.009	2012–6–15	A6IV	8120	10	3.82	0	–0.03	0	–19	1
KIC 5180796	289.95658	40.32186	GDOR	0.5291	0.028	2017–6–13	A6IV	8156.85	5.73	3.81	0.007	–0.004	0.005	–42.23	1
KIC 5294571	296.80221	40.46733	GDOR	0.66934	0.012	2013–10–5	F0	6910	20	4.06	0.03	0.04	0.02	–21	3
KIC 5294571	296.80221	40.46733	GDOR	0.66934	0.012	2014–5–22	F0	6990	30	4.06	0.03	0.03	0.02	–39	3
KIC 5371747	294.43121	40.594	GDOR	0.88652	0.167	2015–10–8	F0	7150	10	4.1	0	–0.17	0	–15	1
KIC 5630362	294.83021	40.89969	GDOR	0.20593	0.027	2015–10–18	A7V	7660	10	3.85	0	–0.13	0	–28	1
KIC 5724048	296.75192	40.93611	GDOR	0.46926	0.009	2014–5–22	F3	6470	100	4.23	0.14	–0.27	0.09	41	7
KIC 5724048	296.75192	40.93611	GDOR	0.46926	0.009	2013–10–5	F3	6540	20	4.2	0.02	–0.26	0.01	17	2
KIC 5724048	296.75192	40.93611	GDOR	0.46926	0.009	2012–6–17	F3	6570	40	4.21	0.05	–0.27	0.03	4	4

Table 2 — *Continued.*

Name	R.A. (deg)	Dec. (deg)	Type	P (d)	Dist	Date	Sp.	T (K)	E_1	$\log(g)$	E_2	[Fe/H]	E_3	$V_{\rm r}$	E_4
KIC 5724048	296.75192	40.93611	GDOR	0.46926	0.082	2015–10–8	F0	6590	10	4.24	0	–0.25	0	9	1
KIC 5772411	284.99829	41.01508	GDOR	1.18624	0.173	2016–5–12	F0	6980	10	4.06	0	–0.09	0	0	1
KIC 6301745	296.464	41.63167	GDOR	2.54453	0.011	2012–6–17	F0	6920	30	4.13	0.03	–0.08	0.02	–21	3
KIC 6519869	291.01358	41.94844	GDOR	0.7391	0.016	2013–9–26	F0	7090	30	4.03	0.03	–0.14	0.02	–20	3
KIC 6519869	291.01358	41.94844	GDOR	0.7391	0.016	2013–5–19	F0	7150	10	4.07	0	–0.09	0	–18	1
KIC 6923424	281.95721	42.441	GDOR	0.36563	0.131	2017–5–14	F0	7057.09	1.37	4.075	0.001	–0.147	0.001	–32.01	0.3
KIC 6923424	281.95721	42.441	GDOR	0.36563	0.005	2013–10–7	F0	7090	10	4.12	0	–0.13	0	–21	1
KIC 7007103	280.98829	42.51825	GDOR	0.64935	1.983	2017–6–7	F0	6997.67	216.9	3.682	0.307	0.146	0.203	–13.73	18.26
KIC 7007103	280.98829	42.51825	GDOR	0.64935	0.039	2017–6–7	F0	7046.14	10.83	3.878	0.007	0.056	0.009	–21.18	2.38
KIC 7007103	280.98829	42.51825	GDOR	0.64935	0.005	2013–10–7	F0	7070	10	4.01	0	0.03	0	–17	1
KIC 7106648	288.16579	42.64458	GDOR	0.42463	0.053	2015–10–11	F0	7270	10	4.07	0	0	0	–15	1
KIC 7106648	288.16579	42.64458	GDOR	0.42463	0.053	2017–6–15	F0	7291.29	7.91	4.053	0.01	0.03	0.008	–11.54	1.14
KIC 7215607	296.0485	42.75264	GDOR	0.44823	0.004	2012–6–4	F0	6850	20	4.13	0.02	0.05	0.01	-3	2
KIC 7220356	297.11729	42.74358	GDOR	0.79302	0.471	2015–10–8	F0	7090	10	3.94	0	0.19	0	–22	1
KIC 7220356	297.11729	42.74358	GDOR	0.79302	0.012	2014–5–22	F0	7100	40	3.91	0.04	0.18	0.03	–8	3
KIC 7220356	297.11729	42.74358	GDOR	0.79302	0.012	2013–10–5	F0	7250	310	3.96	0.44	0.26	0.29	–16	23
KIC 7436266	289.1425	43.02408	GDOR	0.58343	0.094	2016–5–18	F0	6910	300	4.04	0.42	–0.14	0.27	–44	22
KIC 7436266	289.1425	43.02408	GDOR	0.58343	0.011	2013–5–19	F0	7000	10	4.06	0	–0.07	0	–62	1
KIC 7436266	289.1425	43.02408	GDOR	0.58343	0.111	2015–9–25	F0	7010	10	4.02	0	–0.04	0	–52	1
KIC 7436266	289.1425	43.02408	GDOR	0.58343	0.637	2015–10–11	F0	7020	10	4.02	0	–0.05	0	–51	1
KIC 7436266	289.1425	43.02408	GDOR	0.58343	0.111	2017–6–15	F0	7027.22	2.24	4.031	0.001	–0.037	0.002	–45.33	0.49
KIC 7436266	289.1425	43.02408	GDOR	0.58343	0.637	2013–9–26	F0	7040	10	4.05	0	–0.04	0	–45	1
KIC 7694191	295.53871	43.39372	GDOR	0.37622	0.045	2015–10–8	A5V	8140	10	3.79	0	–0.14	0	–2	1
KIC 7742739	287.8205	43.40689	GDOR	0.48614	0.554	2015–9–25	F0	7070	10	4.05	0	–0.18	0	–50	1
KIC 7742739	287.8205	43.40689	GDOR	0.48614	0.094	2016–5–18	F0	7080	10	4.04	0	–0.2	0	–35	1
KIC 7742739	287.8205	43.40689	GDOR	0.48614	0.554	2017–6–15	F0	7088.69	2.16	4.048	0.001	–0.176	0.002	–33.44	0.47
KIC 7767565	296.4125	43.49528	GDOR	0.5015	0.028	2015–10–8	A6IV	7820	10	3.77	0	0.33	0	0	2
KIC 7890526	291.61471	43.68161	GDOR	0.7391	0.226	2015–10–11	F0	7100	10	4.08	0	–0.25	0	–11	1
KIC 7908633	297.27871	43.68967	GDOR	0.35778	0.28	2014–9–13	A6IV	8040	10	3.91	0.01	–0.15	0.01	–12	2
KIC 8104589	294.25342	43.93236	GDOR	1.85874	0.032	2015–9–21	F4	6450	290	4.19	0.4	–0.12	0.26	–2	21
KIC 8104589	294.25342	43.93236	GDOR	1.85874	0.009	2014–9–13	F3	6620	10	4.18	0	–0.13	0	–19	1
KIC 8123127	299.26721	43.92547	GDOR	1.29199	0.009	2013–9–25	F0	7230	10	4.03	0	–0.11	0	–13	1
KIC 8144674	282.08508	44.00344	GDOR	2.02429	0.078	2017–6–7	F0	7277.18	2.09	3.888	0.001	0.046	0.002	–19.04	0.46
KIC 8230025	290.62271	44.1045	GDOR	0.2733	0.005	2013–5–19	F0	7150	10	3.99	0	–0.07	0	–12	1
KIC 8264075	300.86808	44.132	GDOR	0.83264	0.008	2013–10–25	F0	7150	40	4.13	0.04	–0.13	0.03	13	4
KIC 8264075	300.86808	44.132	GDOR	0.83264	0.008	2013–10–17	F0	7190	110	4.04	0.15	–0.13	0.1	21	9
KIC 8264274	300.91529	44.15647	GDOR	0.67431	0.009	2013–9–25	F0	7240	60	4.01	0.08	–0.07	0.05	6	5
KIC 8330056	300.88771	44.20181	GDOR	0.39417	0.015	2013–9–25	F0	7250	30	4.06	0.03	–0.08	0.02	4	3
KIC 8651452	299.97579	44.70517	GDOR	0.41085	0.012	2013–9–25	F0	7130	10	4	0	0.06	0	–6	1
KIC 8838457	298.289	45.09822	GDOR	0.44326	0.007	2013–9–25	F3	6640	10	4.16	0	–0.09	0	10	1
KIC 8838457	298.289	45.09822	GDOR	0.44326	0.029	2015–10–3	F3	6650	10	4.18	0	–0.08	0	11	1
KIC 8871304	285.73721	45.19506	GDOR	1.03093	0.11	2016–5–18	F0	6980	10	4.08	0	–0.13	0	–31	1
KIC 8871304	285.73721	45.19506	GDOR	1.03093	0.45	2017–6–15	F0	7011.23	1.81	4.093	0.001	–0.105	0.002	–31.37	0.45
KIC 9020157	291.18192	45.35033	GDOR	0.81037	0.41	2015–10–2	F0	7040	10	4.05	0	0	0	–27	1
KIC 9147229	288.54829	45.58308	GDOR	0.50403	0.25	2015–10–2	F0	7250	10	4.05	0	–0.1	0	–3	1
KIC 9490042	300.04871	46.09536	GDOR	0.6169	0.006	2013–9–25	F0	7150	10	3.95	0	0.03	0	–38	1
KIC 9594100	294.23329	46.25514	GDOR	0.95057	0.041	2015–10–1	F0	6820	20	4.15	0.02	–0.06	0.01	0	2
KIC 9654789	294.12	46.31089	GDOR	1.00806	0.004	2014–9–13	F0	7030	100	4.05	0.14	–0.11	0.09	–6	8
KIC 9654789	294.12	46.31089	GDOR	1.00806	0.585	2015–10–2	F0	7050	20	4.07	0.02	–0.09	0.01	–2	2
KIC 9655151	294.25492	46.38317	GDOR	0.70522	0.013	2014–5–20	F0	6990	20	4.09	0.02	–0.16	0.02	–18	2
KIC 9655800	294.4715	46.308	GDOR	0.5144	0	2014–9–13	F0	6920	20	4.07	0.02	–0.02	0.01	–14	2
KIC 9716107	294.2365	46.44944	GDOR	0.46468	0.025	2017–6–14	F0	7217.81	40.1	4.125	0.056	–0.171	0.038	0.31	3.7
KIC 9716107	294.2365	46.44944	GDOR	0.46468	0.025	2015–10–1	F0	7250	20	4.06	0.02	–0.16	0.01	–4	2
KIC 9909300	298.36321	46.76097	GDOR	0.66845	0.009	2013–9–25	A9V	7050	10	4.03	0	–0.02	0.01	–15	2
KIC 10069934	289.73392	47.08733	GDOR	0.92421	0.013	2014–5–20	F0	6970	10	4.03	0	0	0	–6	1
KIC 10073601	291.20292	47.04475	GDOR	0.81967	0.007	2014–5–20	F0	7080	10	3.77	0	0.31	0.01	4	2
KIC 10281360	294.66342	47.39014	GDOR	0.50994	0.146	2015–10–1	F0	7300	10	4.04	0	–0.03	0	–29	1
KIC 10281360	294.66342	47.39014	GDOR	0.50994	0.099	2017–5–16	F0	7329.34	1.94	4.009	0.001	–0.066	0.002	–29.95	0.42
KIC 10586837	285.75992	47.81358	GDOR	0.63735	0.013	2014–9–18	F0	7070	10	4.03	0.01	–0.06	0.01	–3	2
KIC 10586837	285.75992	47.81358	GDOR	0.63735	0.147	2014–5–29	F0	7070	10	3.98	0	–0.05	0	–4	1
KIC 10586837	285.75992	47.81358	GDOR	0.63735	0.147	2015–10–6	F0	7070	310	3.95	0.44	–0.18	0.29	–5	24

Table 2 — *Continued.*

Name	R.A. (deg)	Dec. (deg)	Type	P (d)	Dist	Date	Sp.	T (K)	E_1	$\log(g)$	E_2	[Fe/H]	E_3	$V_{\rm r}$	E_4
KIC 10586837	285.75992	47.81358	GDOR	0.63735	0.147	2014–5–29	F0	7080	10	4	0.01	–0.04	0	–4	1
KIC 10586837	285.75992	47.81358	GDOR	0.63735	0.147	2014–5–2	F0	7090	10	3.99	0	–0.05	0	–8	1
KIC 10652134	285.5345	47.92922	GDOR	1.30548	0.007	2014–9–18	F0	7020	350	4.03	0.49	–0.28	0.32	0	25
KIC 10652134	285.5345	47.92922	GDOR	1.30548	0.155	2014–5–2	F0	7030	10	4.04	0	0	0	3	1
KIC 10652134	285.5345	47.92922	GDOR	1.30548	0.155	2014–5–29	F0	7030	10	4.01	0	–0.02	0	4	1
KIC 10652134	285.5345	47.92922	GDOR	1.30548	0.155	2014–5–29	F0	7030	10	4.04	0	0.01	0	5	1
KIC 10652134	285.5345	47.92922	GDOR	1.30548	0.155	2015–10–6	F0	7030	40	4.01	0.04	–0.01	0.03	–2	3
KIC 11612274	292.67308	49.65297	GDOR	0.3937	0.096	2017–5–16	A6IV	7174.91	15.6	4.067	0.021	–0.212	0.015	0.35	1.85
KIC 11612274	292.67308	49.65297	GDOR	0.3937	0.096	2017–5–31	F0	7244.09	34.81	4.069	0.049	–0.188	0.033	1.73	3.19
KIC 12018834	294.70121	50.40383	GDOR	0.56754	0.012	2014–9–17	F0	7190	10	4.02	0	0	0	–32	1
KIC 12018834	294.70121	50.40383	GDOR	0.56754	0.012	2013–9–14	F0	7200	10	4.01	0	–0.02	0	–13	1
KIC 12058428	289.52358	50.55997	GDOR	0.62578	0.01	2014–9–18	F0	7030	10	4.02	0	0.15	0	–30	1
KIC 12058428	289.52358	50.55997	GDOR	0.62578	0.08	2017–5–31	F0	7055.98	5.36	3.993	0.006	0.162	0.005	–34.49	0.99
KIC 12102187	286.00821	50.62397	GDOR	1.07643	0.009	2014–9–18	F0	7040	10	4.05	0	–0.04	0	–27	1
KIC 12102187	286.00821	50.62397	GDOR	1.07643	0.069	2015–5–30	F0	7050	60	4.02	0.08	–0.07	0.05	–30	5
KIC 2710594	290.88882	37.98349	GDOR	0.7378	0.087	2012–6–15	A9V	7140	140	3.94	0.19	0.11	0.12	–32	10
KIC 7746984	289.68823	43.40043	GDOR	0.7398	0.004	2017–6–15	F6	6300.64	5	4.138	0.006	0.024	0.005	–11.16	0.9
KIC 7746984	289.68823	43.40043	GDOR	0.7398	0.004	2015–9–25	F2	6640	10	4.16	0	0.02	0	–21	1
KIC 7746984	289.68823	43.40043	GDOR	0.7398	0.55	2013–10–4	A9V	6830	30	4.19	0.04	–0.01	0.03	–15	3
KIC 3448365	292.64908	38.58796	GDOR	0.6666	0.044	2012–6–15	F0	6940	10	4	0	0.01	0	–107	1
KIC 3448365	292.64908	38.58796	GDOR	0.6666	0.044	2012–6–17	A9V	6990	10	4.06	0	0.03	0	–37	1
KIC 7939065	282.2999	43.7982	GDOR+DSCT:	0.5786	0.107	2017–5–14	F0	7198.6	1.69	4.051	0.001	–0.162	0.001	-24.89	0.37
KIC 8364249	291.3201	44.39632	GDOR	0.535	0.064	2013–9–26	F0	7050	20	4.01	0.03	0.01	0.02	–16	2
KIC 8364249	291.3201	44.39632	GDOR	0.535	0.131	2015–10–11	F0	7060	10	3.99	0	0.01	0	–27	1
KIC 3952623	291.03427	39.01118	GDOR+DSCT	0.389	0.073	2012–6–15	F0	7230	280	3.85	0.39	0.27	0.26	–34	22
KIC 3952623	291.03427	39.01118	GDOR+DSCT	0.389	0.004	2015–10–12	F0	7250	10	4.02	0	0.26	0	–31	1
KIC 8375138	295.19843	44.33662	GDOR+DSCT:	0.4813	0.754	2015-9-21	F0	7080	60	4.03	0.08	–0.09	0.06	-4	6
KIC 4547348	287.0787	39.69348	GDOR	0.8164	0.596	2014–6–2	F0	6990	10	4.09	0	–0.24	0	–5	1
KIC 8378079	296.12753	44.38279	GDOR	1.9033	0	2015–9–21	F0	6920	10	4.05	0.01	–0.35	0.01	–58	2
KIC 8611423	285.8009	44.74307	GDOR	1.2053	0.011	2016–5–18	F0	7040	20	4.06	0.02	–0.1	0.02	–13	3
KIC 8645874	298.46548	44.71927	GDOR+DSCT	0.5412	0.004	2015–10–3	F0	7180	10	3.97	0	0.05	0	–10	1
KIC 8693972	293.68579	44.87334	GDOR	2.0691	0.004	2015–9–21	F0	6840	40	4.08	0.04	–0.03	0.03	–8	3
KIC 8693972	293.68579	44.87334	GDOR	2.0691	0.026	2014–9–13	F0	6880	10	4.07	0.01	–0.04	0.01	3	2
KIC 8739181	285.02518	44.94541	GDOR	1.1621	0.028	2016–5–18	F0	6970	10	4.01	0.01	–0.2	0.01	–1	2
KIC 8739181	285.02518	44.94541	GDOR	1.1621	0.076	2013–10–4	F0	7030	30	4.03	0.03	–0.21	0.02	11	3
KIC 8836473	297.80127	45.02614	GDOR+DSCT	0.531	0.051	2013–10–17	F0	7130	30	3.91	0.04	0.14	0.02	–27	3
KIC 8836473	297.80127	45.02614	GDOR+DSCT	0.531	0.051	2013–10–25	F0	7130	20	3.91	0.01	0.14	0.01	–28	2
KIC 5350598	287.9765	40.56716	GDOR	0.4633	0.007	2017–6–3	F0	7182.66	2.55	4.079	0.002	–0.097	0.002	–0.18	0.64
KIC 9210943	288.5188	45.6525	GDOR	0.4565	0.316	2017–6–15	F0	6989.2	2.25	4.092	0.001	0.013	0.002	–31.09	0.5
KIC 9210943	288.5188	45.6525	GDOR	0.4565	0.02	2013–10–4	F0	7000	10	4.1	0.01	0	0.01	–27	2
KIC 9419694	297.49164	45.95197	GDOR	0.9682	0.038	2013–9–25	F0	7050	20	4.07	0.02	–0.27	0.01	–36	2
KIC 5708550	292.76456	40.93719	GDOR	0.8965	0.064	2012–6–17	F0	6950	90	4.04	0.12	–0.11	0.08	–13	7
KIC 5708550	292.76456	40.93719	GDOR	0.8965	0.219	2015–10–12	F0	6970	10	4.04	0	–0.06	0	–27	1
KIC 5708550	292.76456	40.93719	GDOR	0.8965	0.064	2012–6–15	F0	7070	120	4.14	0.16	–0.06	0.11	–12	10
KIC 5772452	285.01892	41.08811	GDOR	1.4207	0.007	2017–6–3	K0	5224.24	29.29	4.552	0.039	0.166	0.028	–22.29	3.5
KIC 5788623	291.04611	41.01152	GDOR	1.2837	0.05	2012-6-15	F0	7040	70	4.03	0.09	–0.14	0.06	–22	5
KIC 5788623	291.04611	41.01152	GDOR	1.2837	0	2015–10–11	F0	7080	10	4.14	0	–0.15	0	–12	1
KIC 5788623	291.04611	41.01152	GDOR	1.2837	0.05	2013–5–19	A8III	7140	80	4.14	0.11	–0.19	0.07	–22	7
KIC 9751996	281.49786	46.51201	GDOR+DSCT:	0.7785	0.679	2014–5–29	F0	7140	10	3.82	0	0.42	0	–67	1
KIC 6185513	284.371	41.51614	GDOR+DSCT	0.4453	0.171	2016–5–12	F0	7305.57	2.68	4.005	0.002	–0.139	0.002	–31.01	0.6
KIC 6185513	284.371	41.51614	GDOR+DSCT	0.4453	0.171	2017–6–7	F0	7310	10	4.01	0.01	–0.12	0.01	–34	2
KIC 6185513	284.371	41.51614	GDOR+DSCT	0.4453	0.171	2017–6–7	F0	7310	10	4.01	0.01	–0.14	0.01	–27	2
KIC 6185513	284.371	41.51614	GDOR+DSCT	0.4453	0.171	2013–10–7	F0	7310.7	2.37	4.007	0.001	–0.137	0.002	–29.15	0.52
KIC 6185513	284.371	41.51614	GDOR+DSCT	0.4453	0.171	2017–6–7	F0	7319.95	2.73	4.026	0.002	–0.137	0.002	–30.59	0.6
KIC 10080943	294.11375	47.08394	GDOR+DSCT+ELL+R	0.94395	0.186	2013–5–22	F0	7200	20	4.16	0.02	–0.14	0.02	–36	3
KIC 10080943	294.11375	47.08394	GDOR+DSCT+ELL+R	0.94395	0.186	2017–6–14	F0	7222.01	19.96	4.094	0.027	–0.122	0.019	–27.99	2.18
KIC 10080943	294.11375	47.08394	GDOR+DSCT+ELL+R	0.94395	0.186	2017–6–14	F0	7223.29	6.52	4.11	0.007	–0.151	0.006	–29.98	1.15
KIC 10080943	294.11375	47.08394	GDOR+DSCT+ELL+R	0.94395	0.186	2017–6–14	F0	7248.76	7.86	4.1	0.009	–0.149	0.007	–28.9	1.27
KIC 6342398	282.89301	41.7764	GDOR	0.9307	0.007	2017–6–7	F0	7049.44	3.02	4.031	0.002	–0.05	0.003	7.63	0.74
KIC 6342398	282.89301	41.7764	GDOR	0.9307	0.007	2015–10–4	F0	7060	10	4.04	0	–0.04	0	24	1
KIC 10224094	297.52768	47.28516	GDOR	0.9878	0	2015–10–1	F0	7090	10	4.07	0	–0.03	0	–14	1
KIC 6367159	292.8381	41.74875	GDOR+DSCT	1.9059	0.004	2015–10–11	A7V	7310	10	4.09	0	–0.15	0	–15	1

Table 2 — *Continued.*

Name	R.A. (deg)	Dec. (deg)	Type	P (d)	Dist	Date	Sp.	T (K)	E_1	$\log(g)$	E_2	[Fe/H]	E_3	V_r	E_4
KIC 10256787	283.44662	47.39306	GDOR	0.9281	0.019	2014–5–29	A9V	6970	20	4.18	0.02	–0.06	0.01	–8	2
KIC 6425437	285.01373	41.83788	GDOR	1.1151	0.067	2014–6–2	F0	6280	260	3.95	0.36	–0.71	0.23	4	18
KIC 6425437	285.01373	41.83788	GDOR	1.1151	0.038	2016–5–12	F0	6980	10	3.95	0	0.09	0	–25	1
KIC 6425437	285.01373	41.83788	GDOR	1.1151	0.244	2017–6–7	F0	7038.12	2.55	3.991	0.002	0.091	0.002	–28.99	0.56
KIC 10467146	290.52521	47.68037	GDOR	1.0471	0.484	2017–6–14	F0	6980.6	16.07	4.072	0.021	–0.316	0.015	23.42	1.92
KIC 10467146	290.52521	47.68037	GDOR	1.0471	0.033	2014–5–20	F0	7020	10	4.04	0.01	–0.3	0.01	5	2
KIC 6467639	298.40762	41.81806	GDOR+DSCT	0.576	0.02	2014–5–22	F0	7350	90	3.73	0.12	0.06	0.08	–2	7
KIC 11080103	289.70892	48.62053	GDOR	0.8055	0.479	2014–5–20	F0	7030	40	4.11	0.04	–0.36	0.03	–18	4
KIC 11080103	289.70892	48.62053	GDOR	0.8055	0.004	2015–10–2	F0	7080	10	4.12	0.01	–0.32	0.01	–5	2
KIC 11080103	289.70892	48.62053	GDOR	0.8055	0.01	2014–9–29	F0	7140	30	4.09	0.03	–0.29	0.02	–5	3
KIC 11080103	289.70892	48.62053	GDOR	0.8055	0.004	2015–5–29	F0	7170	20	4.12	0.02	–0.27	0.02	–3	2
KIC 11080103	289.70892	48.62053	GDOR	0.8055	0.132	2017–5–31	F0	7346.92	228.76	4.098	0.328	–0.097	0.213	–1.27	17.08
KIC 6468146	298.51767	41.80861	GDOR+DSCT	0.647	0.011	2015–10–8	F0	7180	10	3.97	0	–0.02	0	–34	1
KIC 6468146	298.51767	41.80861	GDOR+DSCT	0.647	0.102	2013–10–5	A8III	7180	20	3.99	0.01	0.01	0.01	–41	2
KIC 11099031	298.15631	48.64556	GDOR+DSCT:	1.0891	0.59	2013–5–22	F3	6800	10	3.86	0	0.3	0	–21	1
KIC 6468987	298.70419	41.80376	GDOR+DSCT:	0.5003	0.004	2015–10–8	F0	7030	10	4.02	0.01	–0.06	0.01	–36	2
KIC 11196370	294.68536	48.84879	GDOR+DSCT:	0.3519	0.084	2017–5–16	F0	7121.88	20.97	3.968	0.029	0.11	0.02	–31.32	2.15
KIC 11196370	294.68536	48.84879	GDOR+DSCT:	0.3519	0.004	2015–10–1	F0	7260	180	3.97	0.25	0.18	0.17	-27	14
KIC 6678174	287.5238	42.16516	GDOR	0.8863	0.004	2015–10–11	F0	7080	10	4.05	0	–0.15	0	–12	1
KIC 6678174	287.5238	42.16516	GDOR	0.8863	0.004	2017–6–15	F0	7105.88	2.41	4.072	0.001	–0.164	0.002	–21.09	0.58
KIC 11294808	290.68915	49.07987	GDOR+DSCT:	0.4495	0.007	2015–5–29	F0	7010	30	3.97	0.03	–0.02	0.02	–8	3
KIC 11294808	290.68915	49.07987	GDOR+DSCT:	0.4495	0.052	2014–9–17	F0	7010	10	4.02	0	0	0	–8	1
KIC 11456474	292.54373	49.34113	GDOR	0.6796	0.215	2014–9–27	F0	6920	30	4.04	0.04	–0.12	0.02	–13	3
KIC 11456474	292.54373	49.34113	GDOR	0.6796	0.215	2014–9–29	F0	6940	10	4.06	0.01	–0.13	0.01	–7	2
KIC 11456474	292.54373	49.34113	GDOR	0.6796	0.215	2015–10–2	F0	6970	10	4.02	0.01	–0.1	0.01	–23	1
KIC 11456474	292.54373	49.34113	GDOR	0.6796	0.215	2015–5–29	F0	6980	20	4.03	0.02	–0.09	0.01	–23	2
KIC 11456474	292.54373	49.34113	GDOR	0.6796	0.215	2015–10–1	F0	7000	20	4.06	0.02	–0.11	0.01	–35	2
KIC 11456474	292.54373	49.34113	GDOR	0.6796	0.215	2015–10–2	F0	7000	10	4.05	0.01	–0.07	0.01	–23	1
KIC 11456474	292.54373	49.34113	GDOR	0.6796	0.215	2013–9–14	F0	7007.58	6.54	4.05	0.008	–0.049	0.006	–14.68	0.99
KIC 11456474	292.54373	49.34113	GDOR	0.6796	0.215	2017–5–16	F0	7010	10	4.03	0	–0.06	0	–13	1
KIC 11456474	292.54373	49.34113	GDOR	0.6796	0.215	2015–10–1	F0	7020	10	4.05	0	–0.09	0	–10	2
KIC 11456474	292.54373	49.34113	GDOR	0.6796	0.215	2017–5–31	F0	7020	10	4.06	0	–0.07	0	–14	1
KIC 6935014	287.1666	42.45327	GDOR	0.8287	0.02	2016–5–18	F0	7060	50	4.04	0.06	0.03	0.04	–3	4
KIC 11668783	295.36426	49.79479	GDOR	1.5924	0.049	2013–9–14	F0	6940	10	4.04	0.01	–0.02	0.01	–34	1
KIC 11668783	295.36426	49.79479	GDOR	1.5924	0.006	2017–5–16	F0	6973.09	10.08	4.053	0.013	–0.019	0.01	–32.52	1.34
KIC 6953103	293.2135	42.47959	GDOR	0.7766	0.025	2014–9–13	F0	7040	20	4.12	0.02	–0.28	0.01	–4	2
KIC 6953103	293.2135	42.47959	GDOR	0.7766	0.004	2015–9–21	F0	7140	50	4.12	0.07	–0.25	0.04	–7	5
KIC 6953103	293.2135	42.47959	GDOR	0.7766	0.025	2012–6–17	F0	7390	370	4.08	0.52	–0.25	0.34	–12	27
KIC 11721304	295.86603	49.85706	GDOR	1.265	0.031	2013–5–22	F0	7080	40	4.07	0.05	–0.03	0.03	–8	4
KIC 11721304	295.86603	49.85706	GDOR	1.265	0.004	2015–10–1	F0	7100	10	4.06	0	–0.05	0	–2	1
KIC 11721304	295.86603	49.85706	GDOR	1.265	0.032	2017–5–16	F0	7116.54	2.62	4.045	0.002	–0.029	0.002	–2.88	0.59
KIC 7023122	288.42526	42.52028	GDOR	0.533	0.04	2015–10–11	F0	7190	10	4.1	0	–0.18	0	–24	1
KIC 7023122	288.42526	42.52028	GDOR	0.533	0.04	2015–10–11	F0	7190	10	4.1	0	–0.19	0	–24	1
KIC 7023122	288.42526	42.52028	GDOR	0.533	0.04	2015–9–25	F0	7210	10	4.1	0	–0.19	0	–33	1
KIC 7023122	288.42526	42.52028	GDOR	0.533	0.04	2015–9–25	F0	7220	10	4.11	0	–0.2	0	–33	1
KIC 7023122	288.42526	42.52028	GDOR	0.533	0.04	2013–10–4	F0	7250	10	4.09	0	–0.19	0	–27	1
KIC 7023122	288.42526	42.52028	GDOR	0.533	0.04	2013–9–26	F0	7260	10	4.1	0	–0.19	0	–19	1
KIC 11754232	286.49136	49.94265	GDOR+DSCT	1.0874	0.479	2015–5–30	F0	7210	20	4.09	0.01	–0.05	0.01	–13	2
KIC 11754232	286.49136	49.94265	GDOR+DSCT	1.0874	0.479	2015–5–30	F0	7210	30	4.13	0.04	–0.06	0.03	–3	3
KIC 11754232	286.49136	49.94265	GDOR+DSCT	1.0874	0.021	2017–5–31	A7IV	7239.42	5.8	4.126	0.006	–0.025	0.005	4.24	1.14
KIC 7365537	292.64682	42.96963	GDOR+DSCT:	0.3418	0.081	2013–9–26	F0	7260	10	4.06	0	–0.06	0	–29	1
KIC 7380501	296.67328	42.99315	GDOR	1.0381	0.562	2014–9–13	F0	6900	170	4.08	0.24	–0.12	0.16	–20	14
KIC 7380501	296.67328	42.99315	GDOR	1.0381	0.004	2015–9–21	F0	6970	60	4.04	0.08	–0.02	0.05	–11	5
KIC 11907454	287.87253	50.24159	GDOR	0.8423	0.081	2017–5–31	F0	6936.65	392.98	4.217	0.562	–0.006	0.366	2.06	29.86
KIC 11907454	287.87253	50.24159	GDOR	0.8423	0.474	2015–5–30	F0	7030	40	4.08	0.04	–0.02	0.03	5	3
KIC 11907454	287.87253	50.24159	GDOR	0.8423	0.037	2014–9–18	F0	7040	10	4.08	0	0	0	7	1

Table 2 — *Continued.*

Name	R.A. (deg)	Dec. (deg)	Type	P (d)	Dist	Date	Sp.	T (K)	E_1	$\log(g)$	E_2	[Fe/H]	E_3	$V_{\rm r}$	E_4
KIC 7434470	288.49142	43.08277	GDOR+DSCT	0.5887	0.049	2016–5–18	F0	6950	10	4.08	0.01	–0.07	0.01	–23	2
KIC 7434470	288.49142	43.08277	GDOR+DSCT	0.5887	0.004	2015–10–11	F0	6970	10	4.12	0	–0.08	0	–27	1
KIC 7434470	288.49142	43.08277	GDOR+DSCT	0.5887	0.03	2013–9–26	F0	6980	10	4.12	0	–0.07	0	–3	1
KIC 11917550	293.59402	50.26286	GDOR	0.7766	0.046	2013–5–22	F0	7090	10	4.06	0.01	0	0.01	3	1
KIC 11920505	294.98795	50.22558	GDOR	0.8342	0.077	2013–5–22	F0	7060	10	4.04	0	–0.02	0	–34	1
KIC 7583663	281.73941	43.27092	GDOR	0.9571	0.015	2017–5–14	F0	6999.99	2.15	4.033	0.001	0.028	0.002	–37.92	0.51
KIC 7583663	281.73941	43.27092	GDOR	0.9571	0	2015–10–4	F0	7000	10	4.08	0	0.05	0	–27	1
KIC 7583663	281.73941	43.27092	GDOR	0.9571	0	2017–6–7	F0	7026.56	2.65	4.056	0.002	0.031	0.002	–32.01	0.64
KIC 12066947	294.26337	50.50567	GDOR+DSCT:	0.3671	0.019	2017–5–16	F0	7216.02	38.95	4.061	0.055	–0.112	0.037	11.29	3.49
KIC 7691618	294.76111	43.317	GDOR	1.2167	0.004	2015–9–21	F0	7000	10	4.1	0.01	–0.22	0.01	–22	2
KIC 12458189	290.20468	51.3359	GDOR+DSCT:	0.9619	0.033	2017–5–31	G7	5527.59	224.96	4.103	0.324	–0.249	0.209	–10.1	16.03
KIC 12643786	288.45502	51.78009	GDOR	0.62	0	2015–5–29	A7IV	7100	10	4.11	0	–0.28	0	–6	1
KIC 3441414	290.84054	38.54961	GDOR	0.81072	1.438	2015–10–12	F0	7070	20	4.03	0.02	–0.13	0.01	–8	2
KIC 3441414	290.84054	38.54961	GDOR	0.81072	1.438	2012–6–15	F0	7080	10	4.04	0	–0.15	0	0	1
KIC 3441414	290.84054	38.54961	GDOR	0.81072	1.438	2012–6–15	F0	7090	10	4.04	0	–0.13	0	–2	1
KIC 3441414	290.84054	38.54961	GDOR	0.81072	1.438	2015–10–12	F0	7100	20	4.05	0.02	–0.1	0.01	–6	2

weight is the inverse square of the original error. The radial velocities $V_{\rm r}$ are not averaged because they were observed at different phases and vary with time.

The temperature distribution is plotted in Figure 4 and the peak is near 7040 K (the red dashed line). This temperature peak corresponds to an F2-type main-sequence star with a stellar mass of about 1.52 $M_{\odot}$ (Cox 2000). Two γ Dor stars, KIC 12458189 and KIC 5772452, are cool stars with temperatures lower than 5600 K. Their spectral types are G7 and K0, respectively. Most of the γ Dor stars have temperatures in the range from 6880 K to 7280 K. This indicates that the majority of γ Dor stars is F0-F3 type stars with masses from 1.48 to 1.60 $M_{\odot}$. Three γ Dor variables, KIC 5180796, KIC 7694171 and KIC 5772452, are A-type stars with temperatures higher than 8000 K.

The distribution of gravitational acceleration $\log(g)$ is displayed in Figure 5 where there is a peak around 4.05. The values of $\log(g)$ for most γ Dor variables are in the range from 3.9 to 4.15, indicating that they are main-sequence stars. The $\log(g)$ values of four γ Dor stars, KIC 6467639, KIC 10073601, KIC 7767565 and KIC 7694191, are smaller than 3.8, indicating that they are giants rather than main-sequence stars. The metallicity ([Fe/H]) distribution is plotted in Figure 6. As shown in the figure, the peak is between [Fe/H]$= -0.09$ and 0.01. Most γ Dor stars are slightly metal poorer than the Sun. This is in agreement with the conclusion proposed by Handler (1999) that γ Dor stars are slightly deficient in metal abundances. Only four γ Dor variables, KIC 9751996, KIC 7767565, KIC 10073601 and KIC 11099031, are high-metallicity stars with metallicities higher than 0.3. This could explain why surveys targeting γ Dor stars in the Hyades cluster ([Me/H] = 0.18) were unsuccessful (e.g., Rodríguez & Breger 2001).

The distribution of radial velocity ($V_{\rm r}$) is displayed in Figure 7 where 255 $V_{\rm r}$ for 137 γ Dor stars are plotted. As shown in the figure, the radial velocities of most γ Dor stars are in the range from $V_{\rm r} = -35$ to $-5\,{\rm km\,s^{-1}}$. The two red dashed lines in the figure refer to the borders of the range, while the red solid line represents the middle with a radial velocity of $V_{\rm r} = -20\,{\rm km\,s^{-1}}$. As reported by Qian et al. (2017, 2018b), the peaks of the radial-velocity distributions for both EAs (EA-type binaries) and EWs (EW-type binaries) are near $V_{\rm r} = -20\,{\rm km\,s^{-1}}$. The distribution peak of $V_{\rm r}$ in $-20\,{\rm km\,s^{-1}}$ can be explained by the peculiar solar motion, which is defined as the Sun's motion with respect to the local standard of rest (Schönrich et al. 2010). However, noting that most of these γ Dor stars are located in the field of the *Kepler* mission, the value $-20\,{\rm km\,s^{-1}}$ should refer to the motion of the *Kepler* stars relative to the Sun. The relation between radial velocity and pulsation period is shown in Figure 8 where the lines refer to the distribution peaks of radial velocity. Those radial velocities are useful for investigating binarity of the observed γ Dor stars.

In the solar neighborhood, about 60%–80% of field stars are in binary or multiple systems (e.g., Duquennoy & Mayor 1991). Some δ Sct stars have been detected to be a member in binary or multiple systems (e.g., Mkrtichian et al. 2003; Soydugan et al. 2006; Li et al. 2010; Li & Qian 2013; Qian et al. 2015; Liakos & Niarchos 2017; Kahraman Aliçavuş et al. 2017; Qian et al. 2018a). A very interesting question is what percent of γ Dor stars is in binaries or multiples. However, investigation of γ Dor type pulsating stars in stellar systems is a relatively new area. The first γ Dor variable in a binary was discovered by Ibanoğlu et al. (2007) where the γ Dor star is the primary component in the eclipsing binary system VZ CVn. Çakırlı

Table 3 Spectral Types of γ Dor Stars Determined by LAMOST

Name	R.A. (deg)	Dec. (deg)	Type	Period (d)	Distance	Date	Sp.
HN Leo	149.6085	27.759	GDOR	0.775377	0.128	2012–4–16	F0
HAT 199-01905	294.03762	39.62858	GDOR+DSCT	1.12152	0.152	2012–6–15	A7V
HAT 199-01905	294.03762	39.62858	GDOR+DSCT	1.12152	0.152	2012–6–17	A7V
HAT 199-01905	294.03762	39.62858	GDOR+DSCT	1.12152	0.067	2015–10–12	A7V
FG CVn	201.10983	30.55394	GDOR	3.3479	0.028	2012–3–7	A7V
NGC 6866 V1	301.04658	44.09258	GDOR+DSCT	0.27571	0.013	2013–9–25	A7V
NGC 6866 V2	301.0165	44.17236	GDOR+DSCT	0.072459	0.004	2013–9–25	A7V
NGC 6866 V12	300.97575	44.11275	GDOR	0.83612	0.109	2013–9–25	A5V
NGC 6866 V12	300.97575	44.11275	GDOR	0.83612	0.058	2017–6–14	A5V
GSC 03565-00674	295.96492	48.80208	GDOR	1.45985	0.013	2013–5–22	A7V
KID 03424493	285.15642	38.50561	GDOR	0.36914	0.009	2014–6–2	A7V
KIC 9595743	294.83011	46.2493	GDOR	0.5781	0.008	2017–5–16	A7IV
KID 7731467	281.75612	43.419	GDOR:	1.105	0.111	2017–6–7	F2
KID 08197761	301.03879	44.07111	GDOR	0.91158	0.046	2017–6–14	A7V
KID 4660665	293.43	39.72794	GDOR:	0.784	0.115	2012–6–15	A7V
KID 4660665	293.43	39.72794	GDOR:	0.784	0.115	2012–6–17	A6IV
KID 6869740	293.77217	42.35561	GDOR	0.3517	1.452	2015–9–21	F0
KID 6869740	293.77217	42.35561	GDOR	0.3517	1.452	2015–9–21	F0
Renson 4413	42.41558	1.06858	GDOR+DSCT	0.046944	0.031	2016–11–23	A7V
HD 247837	87.27	26.256	GDOR	4.28082	0.071	2016–3–3	A6IV
HD 248874	88.59483	30.90053	GDOR	5.64653	0.101	2013–2–26	A0
HD 61659	115.65104	46.49122	GDOR	1.40135	0.043	2015–11–2	A7V
HD 61659	115.65104	46.49122	GDOR	1.40135	0.043	2016–1–22	A7V
HD 61659	115.65104	46.49122	GDOR	1.40135	0.043	2016–2–19	A7V
BD+41 2224	175.37596	40.63964	GDOR	2.85307	0.083	2015–12–29	A1V
BD+35 2465	203.849	35.22753	GDOR	1.31458	0.06	2017–1–29	A7V
BD+35 2465	203.849	35.22753	GDOR	1.31458	0.06	2015–1–12	A7V
BD+35 2465	203.849	35.22753	GDOR	1.31458	0.06	2015–2–6	A7V
KIC 1571152	290.919	37.16522	GDOR	2.53807	0.007	2012–6–15	A9V
KIC 1571152	290.919	37.16522	GDOR	2.53807	0.119	2017–6–13	A8III
KIC 2166218	292.73771	37.50994	GDOR	0.55617	0.057	2015–10–12	M3
KIC 2300165	290.81992	37.66653	GDOR	0.59559	0.292	2012–6–15	A7IV
KIC 2575161	291.32358	37.82367	GDOR	0.44543	0.176	2015–10–12	A7III
KIC 2720582	293.08829	37.98583	GDOR	1.81488	0.114	2017–6–13	F0
KIC 2720582	293.08829	37.98583	GDOR	1.81488	0.012	2012–6–15	A8III
KIC 3331147	288.28229	38.45953	GDOR	0.70077	0.34	2017–6–13	F0
KIC 3331147	288.28229	38.45953	GDOR	0.70077	0.093	2017–6–13	A9V
KIC 3539153	289.88629	38.65136	GDOR	0.4914	0.095	2017–6–13	F5
KIC 3539153	289.88629	38.65136	GDOR	0.4914	0.007	2012–6–15	A2V
KIC 4677684	297.18629	39.79236	GDOR	0.22242	0.007	2012–6–17	A6IV
KIC 5105754	293.62979	40.2935	GDOR	0.59277	0.089	2015–10–18	A7IV
KIC 5113797	295.55258	40.29611	GDOR	0.35261	0.165	2017–6–12	A7III
KIC 5180796	289.95658	40.32186	GDOR	0.5291	0.009	2013–5–23	A6IV
KIC 5180796	289.95658	40.32186	GDOR	0.5291	0.009	2013–9–26	A6IV
KIC 5294571	296.80221	40.46733	GDOR	0.66934	0.167	2017–6–12	A9V
KIC 5630362	294.83021	40.89969	GDOR	0.20593	0.027	2017–6–12	A7V
KIC 5630362	294.83021	40.89969	GDOR	0.20593	0.015	2012–6–17	A7V
KIC 5772411	284.99829	41.01508	GDOR	1.18624	0.086	2017–6–3	F0
KIC 6462033	297.1405	41.83036	GDOR	0.69686	0.004	2013–10–5	B6
KIC 6462033	297.1405	41.83036	GDOR	0.69686	0.004	2014–5–22	B6
KIC 6462033	297.1405	41.83036	GDOR	0.69686	0.08	2015–10–8	B6
KIC 6500578	283.35392	41.98803	GDOR	0.66667	0.039	2017–6–7	A5V
KIC 6923424	281.95721	42.441	GDOR	0.36563	0.279	2017–6–7	A7III
KIC 6923424	281.95721	42.441	GDOR	0.36563	0.131	2016–5–12	A8III
KIC 7106648	288.16579	42.64458	GDOR	0.42463	0.012	2013–9–26	A7IV
KIC 7742739	287.8205	43.40689	GDOR	0.48614	0.004	2013–5–19	F0

Table 3 — *Continued.*

Name	R.A. (deg)	Dec. (deg)	Type	Period (d)	Distance	Date	Sp.
KIC 7890526	291.61471	43.68161	GDOR	0.7391	0.006	2013–5–19	A7IV
KIC 7908633	297.27871	43.68967	GDOR	0.35778	0.28	2014–9–13	A5V
KIC 7908633	297.27871	43.68967	GDOR	0.35778	0.28	2015–9–21	A5V
KIC 7908633	297.27871	43.68967	GDOR	0.35778	0.28	2013–10–5	A6IV
KIC 7908633	297.27871	43.68967	GDOR	0.35778	0.28	2013–10–5	A6IV
KIC 7908633	297.27871	43.68967	GDOR	0.35778	0.28	2015–9–21	A6IV
KIC 7908633	297.27871	43.68967	GDOR	0.35778	0.28	2015–9–21	A6IV
KIC 7908633	297.27871	43.68967	GDOR	0.35778	0.28	2015–10–8	A6IV
KIC 7908633	297.27871	43.68967	GDOR	0.35778	0.28	2015–10–8	A6IV
KIC 7908633	297.27871	43.68967	GDOR	0.35778	0.28	2015–10–8	A6IV
KIC 8144674	282.08508	44.00344	GDOR	2.02429	0.018	2017–5–14	A7IV
KIC 8651452	299.97579	44.70517	GDOR	0.41085	0.05	2015–10–3	A7III
KIC 8871304	285.73721	45.19506	GDOR	1.03093	0.004	2017–6–15	F0
KIC 9490067	300.05358	46.05917	GDOR	0.44643	0.013	2013–9–25	A9V
KIC 9654789	294.12	46.31089	GDOR	1.00806	0.11	2017–5–16	F0
KIC 9909300	298.36321	46.76097	GDOR	0.66845	0.123	2015–10–3	A8III
KIC 10385459	282.08079	47.53544	GDOR	0.38521	0.067	2015–5–20	F0
KIC 10586837	285.75992	47.81358	GDOR	0.63735	0.147	2015–5–20	F0
KIC 10652134	285.5345	47.92922	GDOR	1.30548	0.649	2015–5–30	F0
KIC 11612274	292.67308	49.65297	GDOR	0.3937	0.047	2015–10–1	A6IV
KIC 12058428	289.52358	50.55997	GDOR	0.62578	0.452	2015–5–30	A2V
KIC 12102187	286.00821	50.62397	GDOR	1.07643	0.187	2017–5–31	F5
KIC 7746984	289.68823	43.40043	GDOR	0.7398	0.07	2013–5–19	F0
KIC 7867348	280.16989	43.60475	GDOR+DSCT	0.8548	0.007	2015–10–4	F0
KIC 7867348	280.16989	43.60475	GDOR+DSCT	0.8548	0.007	2017–6–7	A9V
KIC 7939065	282.2999	43.7982	GDOR+DSCT:	0.5786	0.004	2017–6–7	G7
KIC 7939065	282.2999	43.7982	GDOR+DSCT:	0.5786	0.068	2013–10–7	A7IV
KIC 8364249	291.3201	44.39632	GDOR	0.535	0.064	2014–9–13	F0
KIC 8364249	291.3201	44.39632	GDOR	0.535	0	2015–9–21	F0
KIC 4547348	287.0787	39.69348	GDOR	0.8164	0.004	2017–6–3	F9
KIC 4757184	294.65384	39.84058	GDOR	0.7907	0.014	2015–10–18	A6IV
KIC 8836473	297.80127	45.02614	GDOR+DSCT	0.531	0.007	2015–10–3	A2V
KIC 9419694	297.49164	45.95197	GDOR	0.9682	0.004	2015–10–3	F0
KIC 5708550	292.76456	40.93719	GDOR	0.8965	0.004	2017–6–12	K2
KIC 10080943	294.11375	47.08394	GDOR+DSCT+ELL+R	0.94395	0.186	2013–9–14	A7V
KIC 10080943	294.11375	47.08394	GDOR+DSCT+ELL+R	0.94395	0.186	2015–10–1	A7V
KIC 10080943	294.11375	47.08394	GDOR+DSCT+ELL+R	0.94395	0.186	2015–10–1	A7V
KIC 6367159	292.8381	41.74875	GDOR+DSCT	1.9059	0.067	2012–6–17	A7V
KIC 11080103	289.70892	48.62053	GDOR	0.8055	0.479	2015–5–30	F0
KIC 6953103	293.2135	42.47959	GDOR	0.7766	0.338	2013–5–19	F0
KIC 7023122	288.42526	42.52028	GDOR	0.533	0.04	2013–5–19	F9
KIC 7023122	288.42526	42.52028	GDOR	0.533	0.04	2016–5–18	A6IV
KIC 7023122	288.42526	42.52028	GDOR	0.533	0.085	2013–5–23	A6IV
KIC 7365537	292.64682	42.96963	GDOR+DSCT:	0.3418	0.081	2013–5–23	A2V
KIC 7380501	296.67328	42.99315	GDOR	1.0381	0.051	2014–9–13	F0
KIC 12066947	294.26337	50.50567	GDOR+DSCT:	0.3671	0.259	2015–10–1	A6IV
KIC 12643786	288.45502	51.78009	GDOR	0.62	0.807	2014–9–17	A7IV
KIC 12643786	288.45502	51.78009	GDOR	0.62	0.807	2014–9–27	A7IV

& Ibanoglu (2016) listed 11 γ Dor variables in binaries and found correlations between pulsation-orbital periods and pulsation period-$\log g$ for the γ Dor binary members. Three more γ Dor stars in binary systems were later detected by several authors (Çakırlı et al. 2017; Lee 2016; Özdarcan & Dal 2017).

Among the 137 γ Dor pulsating stars that have spectroscopic parameters determined by using LAMOST, 64 of them were observed two times or more. The difference between the lowest and highest radial velocities are derived and are listed in Table 4 where 19 γ Dor stars with $V_{\rm r}$ difference larger than $15\,{\rm km\,s^{-1}}$ are shown. The peak-to-peak radial-velocity amplitude for γ Dor stars is

usually in the range from 2 to 4 km s^{-1} (e.g., Balona et al. 1996; Hatzes 1998; Mathias et al. 2004; De Cat et al. 2006). The LAMOST data were compared by Qian et al. (2018a) with those obtained by using high-resolution spectra compiled from the literature by Frasca et al. (2016). The standard error for radial velocity $V_{\rm r}$ was derived as 11 km s^{-1}. Therefore, those γ Dor stars with $\Delta V_{\rm r} > 15$ km s^{-1} may be components of binary or multiple systems. Moreover, as displayed in Figure 8, the radial velocities for most γ Dor type pulsating stars are around $V_{\rm r} = -20$ km s^{-1}. However, the radial velocities of some γ Dor variables showed very high deviations with values larger than 10 km s^{-1} or smaller than -50 km s^{-1}. They are also candidates of γ Dor stars in binary or multiple systems and are shown in Table 5. Six γ Dor stars, KIC 3448635, KIC 5180796, KIC 5724048, KIC 6342398, KIC 7436266 and KIC 10467146, are listed in both Tables 4 and 5. They have high radial velocity deviations with large $V_{\rm r}$ differences and are the most probable binary systems.

4 SEVERAL STATISTICAL CORRELATIONS FOR γ DOR VARIABLES AND NORMAL δ SCT STARS

The correlation between period and effective temperature T is shown in Figure 9 where γ Dor stars with periods shorter than 1.4 d are plotted as blue dots. Twelve γ Dor stars with orbital period longer than 1.4 d are not displayed in the figure. The normal δ Sct stars observed by LAMOST are also displayed as green dots (Qian et al. 2018a). The periods of three γ Dor stars are shorter than 0.3 d. They are KIC 5630326 (P =0.20593 d), KIC 8230025 (P =0.2733 d) and HAT 199-07893 (P =0.28977 d). The other γ Dor stars overlap the long-period δ Sct variables with period longer than 0.3 d. As we can see in the figure, there is a good correlation between effective temperature and pulsation period for short-period pulsating stars with periods shorter than 0.3 d. The red solid line refers to the relation determined by Qian et al. (2018a). It can be explained in that the hotter δ Sct stars tend to be near the main sequence while cooler variables are more evolved (e.g., Rodríguez et al. 2000). However, there is no such relation for long-period ones (dashed magenta line) including γ Dor variables and long-period δ Sct stars.

It is well known that the correlation between gravitational acceleration and pulsation period is almost universal among radially pulsating variable stars (e.g., Fernie 1995). The relation between period and gravitational acceleration for γ Dor variables and normal γ Dor stars is shown in Figure 10. As plotted in the figure, gravitational acceleration ($\log(g)$) is strongly correlated with pulsation period for short-period variables with $P < 0.3$ d. The longer the pulsation period is, the lower the gravitational acceleration will be. The red solid line represents the correlation determined by Qian et al. (2018a) that can be explained as an evolutionary effect. As a star evolves from zero-age main sequence (ZAMS), both the mean density ρ and gravitational acceleration $\log g$ should decrease. As a result, the pulsation period should increase because of the basic relation, $P\sqrt{\rho/\rho_\odot} = Q$, where Q is the pulsation constant. By analyzing six γ Dor stars in binary systems, Çakırlı & Ibanoglu (2016) found a correlation between pulsation period and gravitational acceleration for γ Dor binary members. However, as shown in Figure 9, there is no such relation for γ Dor variables and long-period δ Sct stars.

The correlation between period and metallicity [Fe/H] is shown in Figure 11 for both γ Dor and normal delta Sct stars. Some stars with periods shorter than 0.15 d are relatively metal poor, and they might be Pop. II SX Phe stars. As displayed in Figures 9 and 10, those pulsating variables including γ Dor and normal delta Sct stars are separated into subgroups according to their period. The short-period variables have period shorter than 0.3 d, and the periods of the long-period ones are longer than this value. The properties of the two subgroups are different. As shown by Qian et al. (2018a), the metallicity is weakly correlated with period for short-period pulsating stars, while no such relation for long-period ones is detected.

By analyzing the LAMOST data, Qian et al. (2018a) found a group of 131 unusual and cool variable stars (UCVs) that are cooler than normal δ Sct stars (NDSTs) with pulsation periods in the range from 0.09 to 0.22 d. Among the 137 γ Dor stars observed by LAMOST, 93 were also observed by *Gaia* (Gaia Collaboration et al. 2016b). Their apparent magnitudes and parallaxes were listed in *Gaia* Data Release 1 (Gaia Collaboration, Gaia Collaboration et al. 2016a). The H-R diagram for those γ Dor stars is plotted in Figure 12 (blue dots) where the effective temperature are from LAMOST, while the photometric absolute magnitudes are determined by using the *Gaia* and LAMOST data. Also shown as green dots are long-period NDSTs with periods longer than 0.3 d. For comparison, short-period NDSTs (magenta dots) and UCVs (red dots) are displayed in the figure. The red star stands for the Sun. The red dashed lines in Figure 12 refer to the blue and red edges of γ Dor stars from Handler (1999), while the blue dashed lines to those edges from McNamara (2000) for δ Sct stars. The ZAMS from Kippenhahn et al. (2012) is plotted as a green line. The

Table 4 19 γ Dor Stars with Radial Velocity Difference Larger Than 15 km s^{-1}

Name	P (d)	Dates	Times	T (K)	$\log(g)$	[Fe/H]	$V_{\rm High}$	$V_{\rm Low}$	$\Delta V_{\rm r}$
KIC 3448365	0.6666	2012–06–15–2012–06–17	2	6965	4.03	0.02	−107	−37	70
KIC 5724048	0.46926	2012–06–17–2015–10–08	4	6578	4.21	−0.26	4	41	37
KIC 5180796	0.5291	2012–06–15–2017–06–13	3	8136	3.81	−0.01	−54	−19	35
KIC 6425437	1.1151	2014–06–02–2017–06–07	3	7034	3.99	0.09	−28.99	4	32.99
KIC 11456474	0.6796	2013–05–22–2017–05–31	10	6995	4.05	−0.08	−35	−7	28
KIC 7434470	0.5887	2013–09–26–2016–05–18	3	6966	4.08	−0.07	−27	−3	24
KIC 12018834	0.56754	2013–09–14–2014–09–17	2	7195	4.01	−0.01	−32	−13	19
KIC 4069477	0.71023	2015–10–18–2017–06–12	2	7096	4.05	−0.07	−42.74	−24	18.74
KIC 10467146	1.0471	2014–05–20–2017–06–14	2	7009	4.05	−0.3	5	23.42	18.42
KIC 7436266	0.58343	2013–05–19–2017–06–15	6	7025	4.03	−0.04	−62	−44	18
KIC 5294571	0.66934	2013–10–05–2014–05–22	2	6934	4.06	0.04	−39	−21	18
KIC 11754232	1.0874	2015–05–30–2017–05–31	3	7236	4.12	−0.03	−13	4.24	17.24
KIC 8104589	1.85874	2014–09–13–2015–09–21	2	6619	4.18	−0.13	−19	−2	17
KIC 11080103	0.8055	2014–05–20–2017–05–31	5	7098	4.12	−0.31	−18	−1.27	16.73
KIC 7742739	0.48614	2015–09–25–2017–06–15	3	7087	4.05	−0.18	−50	−33.44	16.56
KIC 4164363	0.72411	2015–10–18–2017–06–12	2	7336	4.04	−0.06	−22.47	−6	16.47
KIC 6342398	0.9307	2015–10–04–2017–06–07	2	7050	4.03	−0.05	7.63	24	16.37
KID 6869740	0.3517	2012–06–04–2015–10–18	5	7084	3.99	0.06	−39	−23	16
KIC 5708550	0.8965	2012–06–15–2015–10–12	3	6970	4.04	−0.07	−27	−12	15

Table 5 20 γ Dor Variable Stars with Radial Velocity Larger Than 10 km s^{-1} or Smaller Than –50 km s^{-1}

Name	Period (d)	Sp.	T (K)	$\log(g)$	[Fe/H]	$V_{\rm r}$ (km s^{-1})
KIC 3448365	0.6666	F0	6940	4.00	0.01	−107
KIC 9751996	0.7785	F0	7140	3.82	0.42	−67
KIC 7436266	0.58343	F0	7000	4.06	−0.07	−62
ASAS J025657+1848.5	1.01077	F0	7090	4.09	−0.03	−59
KIC 2720582	1.81488	F0	7070	4.02	−0.01	−58
KIC 8378079	1.9033	F0	6920	4.05	−0.35	−58
KIC 2720582	1.81488	F0	7030	4.03	−0.04	−56
KIC 5180796	0.5291	A5V	8090	3.80	−0.04	−54
KIC 3327681	0.98912	F5	6554.01	4.093	−0.007	−53.76
KIC 7436266	0.58343	F0	7010	4.02	−0.04	−52
KIC 7436266	0.58343	F0	7020	4.02	−0.05	−51
KIC 7742739	0.48614	F0	7070	4.05	−0.18	−50
KIC 5724048	0.46926	F3	6470	4.23	−0.27	41
HAT 199−01905	1.12152	A6IV	7254.6	4.169	−0.296	27.13
KIC 6342398	0.9307	F0	7060	4.04	−0.04	24
KIC 10467146	1.0471	F0	6980.6	4.072	−0.316	23.42
KIC 8264075	0.83264	F0	7190	4.04	−0.13	21
NSV 16957	1.488	F2	6170	3.89	0.02	20
KIC 3215800	0.66401	F5	6390	4.2	−0.27	19
KIC 5724048	0.46926	F3	6540	4.2	−0.26	17
KIC 8264075	0.83264	F0	7150	4.13	−0.13	13
KIC 12066947	0.3671	F0	7216.02	4.061	−0.112	11.29
KIC 8838457	0.44326	F3	6650	4.18	−0.08	11
KIC 8739181	1.1621	F0	7030	4.03	−0.21	11
NSV 20738	1.38688	A3V	7060.05	4.21	−0.512	10.35
KIC 8838457	0.44326	F3	6640	4.16	−0.09	10

solid blue and red lines represent the blue and red edges for δ Sct and γ Dor stars given by Xiong et al. (2016), respectively.

We can see in Figure 12 that most γ Dor stars lie in a small region where most long-period NDSTs are also located. This region is inside the blue and red edges given by Handler (1999). However, some γ Dor variables are beyond the two edges. Theoretical investigation by Xiong et al. (2016) revealed that oscillations of both δ Sct and γ Dor pulsating stars are caused by the combination of the κ mechanism and coupling between convection and oscillations. The borders for γ Dor stars given by these au-

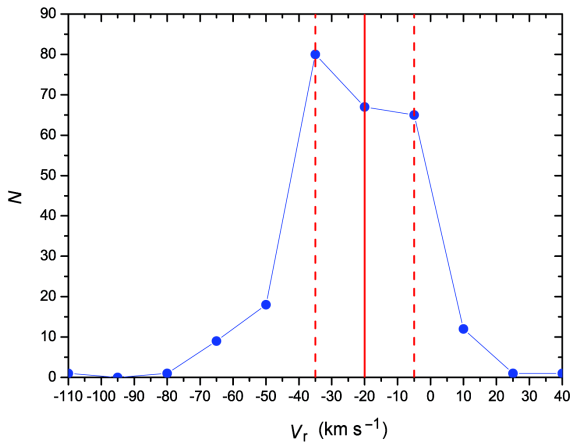

Fig. 7 The distribution of radial velocity V_r for those γ Dor stars observed by LAMOST. The peaks are from $V_r = -35$ to $-5\,\mathrm{km\,s^{-1}}$.

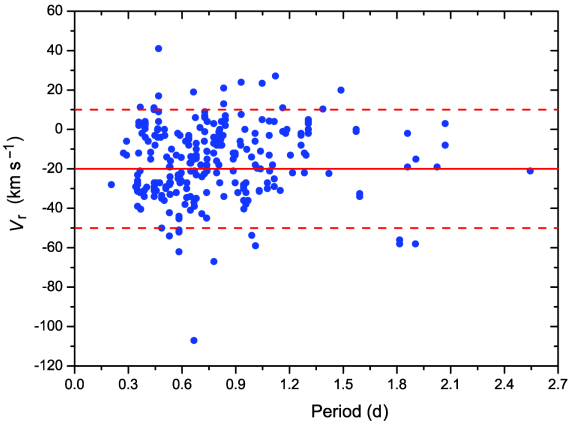

Fig. 8 The correlation between pulsation period and radial velocity. The *solid line* refers to the peak of the radial velocity distribution, while the two *dashed lines* represent the two borders of the peak.

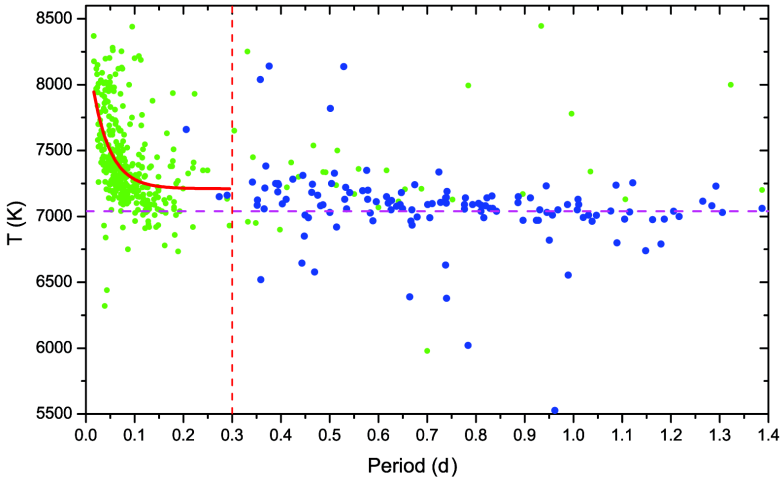

Fig. 9 The correlation between effective temperature and pulsation period for the γ Dor stars observed by LAMOST (*blue dots*). For comparison, the normal LAMOST δ Sct stars are also shown as *green dots*. The *red solid line* refers to the relation for short-period δ Sct stars with periods shorter than 0.3 d determined by Qian et al. (2018a). The *red dashed line* represents the border between the short- and long-period pulsating stars in the lower part of the instability strip on the H-R diagram. It is evident that effective temperature is not correlated with pulsation period for long-period pulsating stars (*dashed magenta line*).

thors are wider. In particular, their red edge could explain all gamma Dor stars in the red region. The δ Sct red edge calculated by Xiong et al. (2016) could also be used to interpret the presence of some UCVs. However, some are still beyond the blue edge of the γ Dor instability strip and red edges of the γ Dor instability strip, indicating that our understanding of the driving mechanisms of these stars is incomplete.

5 DISCUSSION AND CONCLUSIONS

In the past several years, the number of γ Dor stars has enormously increased because of the contributions of several space missions such as *MOST* (Walker et al. 2003), *CoRoT* (Baglin et al. 2006) and *Kepler* (Borucki et al. 2010). These space telescopes led to the discovery of a lot of new γ Dor variables and provided a large amount of high-precision photometric observations. However, the corresponding spectroscopic data are scarce because of the lack of a spectroscopic survey. One-hundred sixty-eight γ Dor variables were observed in the LAMOST spectral survey during the time interval between 2011 October 24 and 2017 June 16. The spectral types of the 168 δ Sct stars are given and stellar atmospheric parameters for 137 targets are presented. One-hundred eleven γ Dor stars were observed by both *Kepler* and LAMOST. The LASP data of

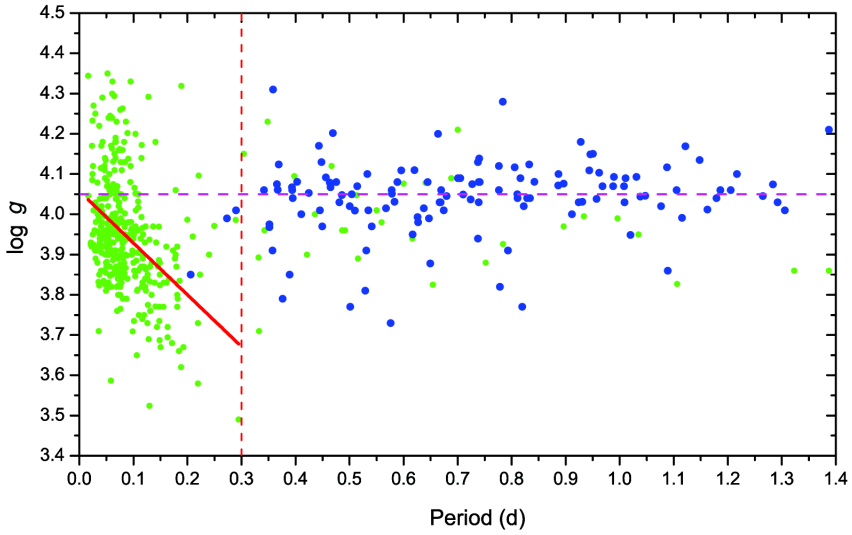

Fig. 10 The correlation between gravitational acceleration and pulsation period for both γ Dor and δ Sct stars. Symbols are the same as those in Fig. 9. The *red dashed line* refers to the border between short- and long-period pulsating stars. It is shown that there is a good correlation between gravitational acceleration and period for short-period pulsating stars with periods shorter than 0.3 d, but there is no such relation for long-period ones (*dashed magenta line*).

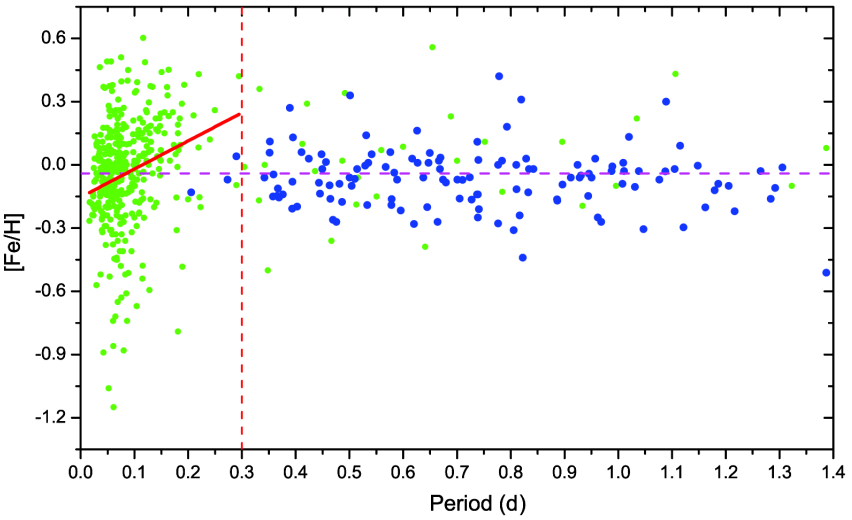

Fig. 11 The same as those in Figs. 9 and 10 but for the correlation between metallicity and pulsation period. The limit of $P = 0.3$ d is set for the separation of the two subgroups, i.e., the short- and long-period pulsating stars.

the 111 γ Dor variables in the LAMOST-*Kepler* field are compared with those derived by Frasca et al. (2016) with the code ROTFIT. It is shown that the LASP values are in a good agreement with those ROTFIT data. Their differences are 200 K for T, 0.2 for $\log g$ and [Fe/H], and 15 km s^{-1} for $V_{\rm r}$. By analyzing 12 γ Dor stars observed four times or more, we obtain that the standard errors for the effective temperature, gravitational acceleration and metallicity are usually lower than 70 K, 0.04 dex and 0.06 dex, respectively.

As listed in Table 4, the radial-velocity differences of 19 γ Dor stars are larger than 15 km s^{-1} among 64 γ Dor variables that were observed twice or more by LAMOST. These results reveal that they may be the γ Dor components in binary systems. Moreover, the radial velocities of 20 γ Dor stars showed large deviations from the peak of the radial-velocity distribution. They are also candidates of γ Dor binary systems. Six γ Dor stars, KIC 3448635, KIC 5180796, KIC 5724048, KIC 6342398, KIC 7436266 and KIC 10467146, have

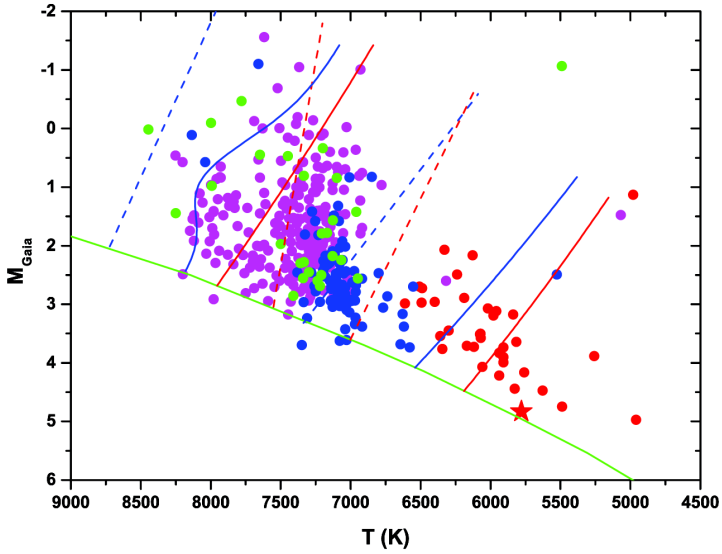

Fig. 12 The H-R diagram for γ Dor variable stars observed by both LAMOST and *Gaia*. *Blue dots* refer to γ Dor stars, while *green dots* to long-period δ Sct variables with period longer than 0.3 d. For comparison, normal short-period δ Sct stars (*magenta dots*) and the new group of variables (*red dots*) detected by Qian et al. (2018a) are also shown. The Sun is plotted as a red star. The *red dashed lines* represent the blue and red edges of γ Dor stars from Handler (1999), while the *blue dashed lines* represent those edges of δ Sct stars from McNamara (2000). The *green line* stands for ZAMS from Kippenhahn et al. (2012). The *solid blue* and *red lines* refer to the blue and red edges for δ Sct and γ Dor stars given by Xiong et al. (2016), respectively.

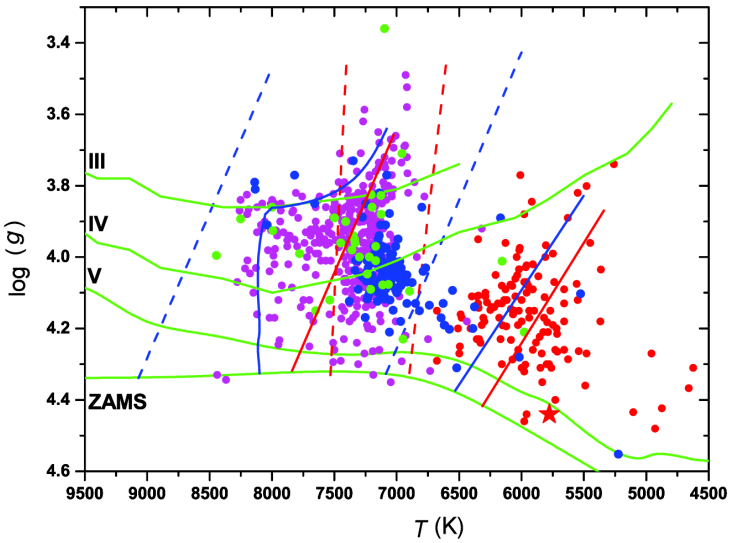

Fig. 13 The $\log g - T$ diagram for γ Dor variable stars observed by LAMOST. Symbols are the same as those in Fig. 12. The *dashed red lines* represent the blue and red edges of the instability strips for γ Dor stars from Handler (1999), while the *dashed blue lines* represent the blue and red edges for δ Sct stars from Rodríguez & Breger (2001). The *green lines* stand for luminosity classes from III to V that are from Straizys & Kuriliene (1981), while the ZAMS line is from Cox (2000). As those plotted in Fig. 12, the *solid red* and *blue lines* refer to the blue and red edges for γ Dor and δ Sct stars determined by Xiong et al. (2016), respectively.

both higher radial-velocity deviations and larger V_r differences. They are the most probable γ Dor binary stars. Some of those γ Dor systems may be eclipsing binaries with high orbital inclinations. New photometric and spectroscopic observations are needed to confirm them in the future. The g-mode pulsations of γ Dor stars are high-order non-radial cases (e.g., Balona et al. 1996; Hatzes 1998). When γ Dor stars are members of close binaries, gravitational effects of close companions may be important for influencing the non-radial pulsations through tidal interactions (e.g., Szatmary 1990). These binaries provide a good

astrophysical laboratory to study the influence of tidal interactions on stellar pulsation.

The relation between $\log(g)$ and T for all γ Dor stars observed by LAMOST is shown in Figure 13 where symbols are the same as those plotted in Figure 12. The dashed red lines are the blue and red edges for γ Dor variables from Handler (1999), while the dashed blue lines refer to the blue and red edges of the instability strips for δ Sct stars from Rodríguez & Breger (2001). The green lines stand for the ZAMS and the luminosity classes range from III to V that are from Cox (2000) and Straizys & Kuriliene (1981), respectively. As displayed in Figures 4 and 6, most of the γ Dor stars have temperatures in the range from 6880 K to 7280 K with metallicities similar to that of the Sun. Their spectral types are from F3 to F0 with masses from 1.48 to 1.60 $M_{\odot}$. This can be seen directly from Figures 12 and 13 where most γ Dor stars occupy a small region in the blue and red edges from Handler (1999) where most long-period NDSTs are also located. The distribution of gravitational acceleration $\log(g)$ shown in Figure 5 indicates that most γ Dor variables are main-sequence stars, but some of them are subgiants or giants. As can be clearly seen in Figure 13, most γ Dor variables are main-sequence stars between ZAMS and IV. However, the luminosity classes of some γ Dor stars are in the range between III and V or between II and III, indicating that these stars evolved from ZAMS. As for δ Sct stars, most of them are subgiants with a range of luminosity classes from IV to III (the distribution peak of $\log(g)$ is 3.91), while some are main-sequence stars or giants (Qian et al. 2018a).

By analyzing *Kepler* data, Uytterhoeven et al. (2011) found that some γ Dor and δ Sct stars are beyond the edges of current observational instability strips. Bradley et al. (2015) investigated the *Kepler* light curves of 2768 stars and discovered 207 γ Dor, 84 δ Sct and 32 hybrid candidate stars. They pointed out that many of those stars are cooler than the red edge of the γ Dor instability strip and a few γ Dor candidate stars lie on the blue side of the ground-based γ Dor instability strip. These properties could be also seen in Figures 12 and 13 where γ Dor and δ Sct variables are beyond the blue and red edges of their instability strips. As pointed out by Balona & Dziembowski (2011), there is a gap between ZAMS and the position of δ Sct stars in the H-R diagram, and the gap increases with growing effective temperature. As shown in Figures 12 and 13, these properties also exist. Moreover, the distribution of pulsating stars turns right around $\log(g) = 3.8$ and $T = 8200$ K with luminosity class around III. It is very interesting that these complex distributions could be interpreted by the theory of Xiong et al. (2016) (the blue lines). However, as shown in the two figures, some pulsating stars occupy a broader region than current stellar pulsation theory predicts. This indicates that our understanding of the physical mechanisms driving stellar structure and pulsations is still incomplete.

Recently, a large number of hybrid stars were reported where both types of pulsation modes were shown. Most of them were found from space missions, especially *Kepler* (e.g., Grigahcène et al. 2010; Catanzaro et al. 2011; Balona et al. 2011; Bradley et al. 2015). It is pointed out by several investigators that there are no pure δ Sct or γ Dor pulsating stars and essentially all of the stars show frequencies in both the δ Sct and γ Dor frequency range (e.g., Grigahcène et al. 2010; Catanzaro et al. 2011; Balona 2014). Hybrid stars occupy the whole region within the γ Dor and δ Sct instability strips and beyond (e.g., Uytterhoeven et al. 2011). As displayed in Figures 12 and 13, both the γ Dor and δ Sct stars also cover the same entire region in the H-R and $\log g - T$ diagrams.

The correlations between period and effective temperature T, gravitational acceleration $\log(g)$ and metallicity [Fe/H] are displayed in Figures 9–11. As displayed in these three figures, γ Dor stars are located in the same region as long-period NDSTs with period longer than 0.3 d and they overlap. The effective temperature T, gravitational acceleration $\log(g)$ and metallicity [Fe/H] are all correlated with the pulsation period for short-period variables. The temperature rapidly decreases when the period increases, but there is no such relation for γ Dor stars or long-period NDSTs. Both the gravitational acceleration and metallicity are found to decrease linearly as the period increases for short-period pulsating stars. However, there are no such relations between pulsation period and those stellar atmospheric parameters for long-period variable stars with periods longer than 0.3 d. These relations reveal that the pulsating variables including γ Dor and normal δ Sct stars are separated in the two subgroups according to their periods. The limit of $P = 0.3$ d is the separation of the two subgroups. These characteristics indicate that the observational properties of the two subgroups are different. The short-period variables (mainly δ Sct stars) pulsate in both radial and non-radial p modes and g modes, while the long-period ones including γ Dor stars and long-period NDSTs may show non-radial high-order g modes (Kaye et al. 1999). Both the γ Dor stars and long-period NDSTs have similar physical properties.

Acknowledgements The Guo Shou Jing Telescope (the Large Sky Area Multi-Object Fiber Spectroscopic Telescope, LAMOST) is a National Major Scientific Project built by the Chinese Academy of Sciences.

Funding for the project has been provided by the National Development and Reform Commission. LAMOST is operated and managed by National Astronomical Observatories, Chinese Academy of Sciences. Spectroscopic observations used in the paper were obtained with LAMOST from 2011 October 24 to 2017 June 16. This work has made use of data from the European Space Agency (ESA) mission *Gaia* (*https://www.cosmos.esa.int/gaia*), processed by the Gaia Data Processing and Analysis Consortium (DPAC, *https://www.cosmos.esa.int/web/gaia/dpac/consortium*). Funding for the DPAC has been provided by national institutions, in particular the institutions participating in the *Gaia* Multilateral Agreement.

References

Aerts, C., Cuypers, J., De Cat, P., et al. 2004, A&A, 415, 1079
Baglin, A., Auvergne, M., Barge, P., et al. 2006, in ESA Special Publication, 1306, The CoRoT Mission Pre-Launch Status - Stellar Seismology and Planet Finding, eds. M. Fridlund, A. Baglin, J. Lochard, & L. Conroy, 33
Balona, L. A., Krisciunas, K., & Cousins, A. W. J. 1994, MNRAS, 270, 905
Balona, L. A., Böhm, T., Foing, B. H., et al. 1996, MNRAS, 281, 1315
Balona, L. A., & Dziembowski, W. A. 2011, MNRAS, 417, 591
Balona, L. A., Guzik, J. A., Uytterhoeven, K., et al. 2011, MNRAS, 415, 3531
Balona, L. A. 2014, MNRAS, 437, 1476
Borucki, W. J., Koch, D., Basri, G., et al. 2010, Science, 327, 977
Bradley, P. A., Guzik, J. A., Miles, L. F., et al. 2015, AJ, 149, 68
Breger, M., & Beichbuchner, F. 1996, A&A, 313, 851
Çakırlı, Ö., & Ibanoglu, C. 2016, New Astron., 45, 36
Çakırlı, Ö., Ibanoglu, C., Sipahi, E., & Akan, M. C. 2017, New Astron., 52, 96
Catanzaro, G., Ripepi, V., Bernabei, S., et al. 2011, MNRAS, 411, 1167
Cousins, A. W. J., & Warren, P. R. 1963, Monthly Notes of the Astronomical Society of South Africa, 22, 65
Cox, A. N. 2000, Allen's astrophysical quantities, 4th ed. (New York: AIP Press)
Cui, X.-Q., Zhao, Y.-H., Chu, Y.-Q., et al. 2012, RAA (Research in Astronomy and Astrophysics), 12, 1197
De Cat, P., Eyer, L., Cuypers, J., et al. 2006, A&A, 449, 281
Dupret, M.-A., Grigahcène, A., Garrido, R., Gabriel, M., & Scuflaire, R. 2005, A&A, 435, 927
Duquennoy, A., & Mayor, M. 1991, A&A, 248, 485
Fernie, J. D. 1995, AJ, 110, 2361
Frasca, A., Alcalá, J. M., Covino, E., et al. 2003, A&A, 405, 149
Frasca, A., Guillout, P., Marilli, E., et al. 2006, A&A, 454, 301
Frasca, A., Molenda-Żakowicz, J., De Cat, P., et al. 2016, A&A, 594, A39
Gaia Collaboration, Brown, A. G. A., Vallenari, A., et al. 2016a, A&A, 595, A2
Gaia Collaboration, Prusti, T., de Bruijne, J. H. J., et al. 2016b, A&A, 595, A1
Grigahcène, A., Dupret, M.-A., Gabriel, M., Garrido, R., & Scuflaire, R. 2005, A&A, 434, 1055
Grigahcène, A., Antoci, V., Balona, L., et al. 2010, ApJ, 713, L192
Guo, Z., Gies, D. R., Matson, R. A., & García Hernández, A. 2016, ApJ, 826, 69
Guzik, J. A., Kaye, A. B., Bradley, P. A., Cox, A. N., & Neuforge, C. 2000, ApJ, 542, L57
Handler, G. 1999, MNRAS, 309, L19
Handler, G. 2009, MNRAS, 398, 1339
Handler, G., & Shobbrook, R. R. 2002, MNRAS, 333, 251
Hatzes, A. P. 1998, MNRAS, 299, 403
Henry, G. W., & Fekel, F. C. 2005, AJ, 129, 2026
Henry, G. W., Fekel, F. C., & Henry, S. M. 2005, AJ, 129, 2815
Henry, G. W., Fekel, F. C., & Henry, S. M. 2007, AJ, 133, 1421
Henry, G. W., Fekel, F. C., & Henry, S. M. 2011, AJ, 142, 39
Ibanoglu, C., Çakırlı, Ö., & Sipahi, E. 2018, New Astron., 62, 70
Ibanoğlu, C., Taş, G., Sipahi, E., & Evren, S. 2007, MNRAS, 376, 573
Kahraman Aliçavuş, F., Soydugan, E., Smalley, B., & Kubát, J. 2017, MNRAS, 470, 915
Kaye, A. B., Handler, G., Krisciunas, K., Poretti, E., & Zerbi, F. M. 1999, PASP, 111, 840
Kippenhahn, R., Weigert, A., & Weiss, A. 2012, Stellar Structure and Evolution (Berlin: Springer-Verlag)
Koleva, M., Prugniel, P., Bouchard, A., & Wu, Y. 2009, A&A, 501, 1269
Krisciunas, K., & Handler, G. 1995, Information Bulletin on Variable Stars, 4195
Krisciunas, K., Aspin, C., Geballe, T. R., et al. 1993, MNRAS, 263, 781
Lee, J. W. 2016, ApJ, 833, 170
Li, L.-J., & Qian, S.-B. 2013, PASJ, 65, 116
Li, L.-J., Qian, S.-B., & Xiang, F.-Y. 2010, PASJ, 62, 987
Liakos, A., & Niarchos, P. 2017, MNRAS, 465, 1181
Luo, A.-L., Zhao, Y.-H., Zhao, G., et al. 2015, RAA (Research in Astronomy and Astrophysics), 15, 1095
Mantegazza, L., Poretti, E., & Zerbi, F. M. 1994, MNRAS, 270, 439
Mathias, P., Le Contel, J.-M., Chapellier, E., et al. 2004, A&A, 417, 189
McNamara, D. H. 2000, in Astronomical Society of the Pacific Conference Series, 210, Delta Scuti and Related Stars, eds. M. Breger & M. Montgomery, 373
Mkrtichian, D. E., Nazarenko, V., Gamarova, A. Y., et al. 2003, in Astronomical Society of the Pacific Conference Series, 292, Interplay of Periodic, Cyclic and Stochastic Variability

in Selected Areas of the H-R Diagram, ed. C. Sterken, 113
Özdarcan, O., & Dal, H. A. 2017, PASA, 34, e017
Poretti, E., Alonso, R., Amado, P. J., et al. 2005, AJ, 129, 2461
Prugniel, P., & Soubiran, C. 2001, A&A, 369, 1048
Qian, S.-B., Li, L.-J., Wang, S.-M., et al. 2015, AJ, 149, 4
Qian, S.-B., He, J.-J., Zhang, J., et al. 2017, RAA (Research in Astronomy and Astrophysics), 17, 087
Qian, S.-B., Li, L.-J., He, J.-J., et al. 2018a, MNRAS, 475, 478
Qian, S.-B., Zhang, J., He, J.-J., et al. 2018b, ApJS, 235, 5
Rodríguez, E., López-González, M. J., & López de Coca, P. 2000, A&AS, 144, 469
Rodríguez, E., & Breger, M. 2001, A&A, 366, 178
Rodríguez, E., Costa, V., Zhou, A.-Y., et al. 2006, A&A, 456, 261
Samadi Ghadim, A., Lampens, P., & Jassur, M. 2018, MNRAS, 474, 5549
Samus', N. N., Kazarovets, E. V., Durlevich, O. V., Kireeva, N. N., & Pastukhova, E. N. 2017, Astronomy Reports, 61, 80
Sarro, L. M., Debosscher, J., Neiner, C., et al. 2013, A&A, 550, A120
Schönrich, R., Binney, J., & Dehnen, W. 2010, MNRAS, 403, 1829
Soydugan, E., İbanoğlu, C., Soydugan, F., Akan, M. C., & Demircan, O. 2006, MNRAS, 366, 1289
Straizys, V., & Kuriliene, G. 1981, Ap&SS, 80, 353
Szatmary, K. 1990, Journal of the American Association of Variable Star Observers (JAAVSO), 19, 52
Tkachenko, A., Aerts, C., Yakushechkin, A., et al. 2013, A&A, 556, A52
Uytterhoeven, K., Mathias, P., Poretti, E., et al. 2008, A&A, 489, 1213
Uytterhoeven, K., Moya, A., Grigahcène, A., et al. 2011, A&A, 534, A125
Walker, G., Matthews, J., Kuschnig, R., et al. 2003, PASP, 115, 1023
Wang, S.-G., Su, D.-Q., Chu, Y.-Q., Cui, X., & Wang, Y.-N. 1996, Appl. Opt., 35, 5155
Watson, C. L., Henden, A. A., & Price, A. 2006, Society for Astronomical Sciences Annual Symposium, 25, 47
Wu, Y., Singh, H. P., Prugniel, P., Gupta, R., & Koleva, M. 2011a, A&A, 525, A71
Wu, Y., Luo, A.-L., Li, H.-N., et al. 2011b, RAA (Research in Astronomy and Astrophysics), 11, 924
Wu, Y., Du, B., Luo, A., Zhao, Y., & Yuan, H. 2014, in IAU Symposium, 306, Statistical Challenges in 21st Century Cosmology, ed. A. Heavens, J.-L. Starck, & A. Krone-Martins, 340
Xiong, D. R., Deng, L., Zhang, C., & Wang, K. 2016, MNRAS, 457, 3163
Zhang, X. B., Deng, L. C., & Luo, C. Q. 2012, AJ, 144, 141
Zhao, G., Zhao, Y.-H., Chu, Y.-Q., Jing, Y.-P., & Deng, L.-C. 2012, RAA (Research in Astronomy and Astrophysics), 12, 723